

**CALOR 2024**  
Tsukuba



# Point Cloud Deep Learning Methods for Particle Shower Reconstruction in the DHCAL

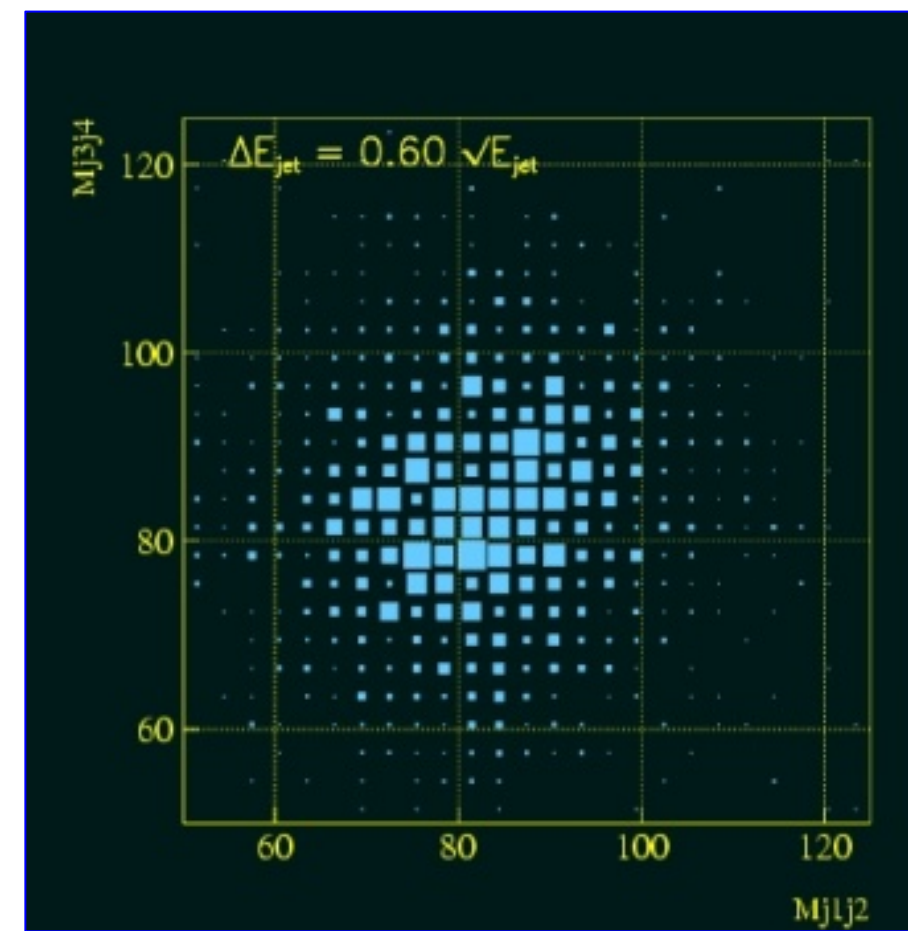
M.Borysova, S. Bressler, E. Gross, N.Kakati, D. Zavazieva  
Weizmann Institute of Science

CALOR24, 19–24 May 2024

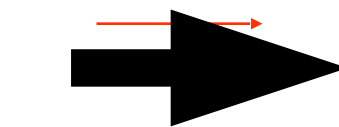
# Digital Hadron Calorimetry

- Hadronic sampling calorimeter
- Designed for future electron-positron colliders (ILC or CEPC)

Future accelerator experiments pose stringent requirements on their detectors

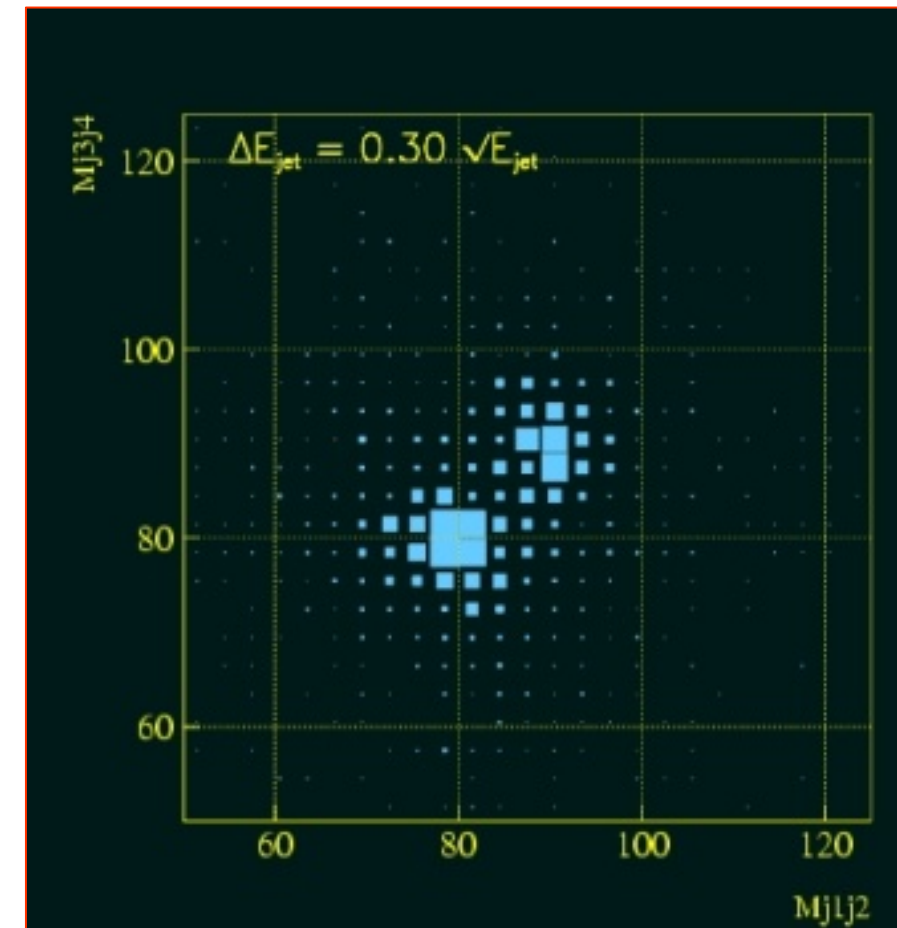


~60%/√E  
Best JET resolution with traditional calorimetry



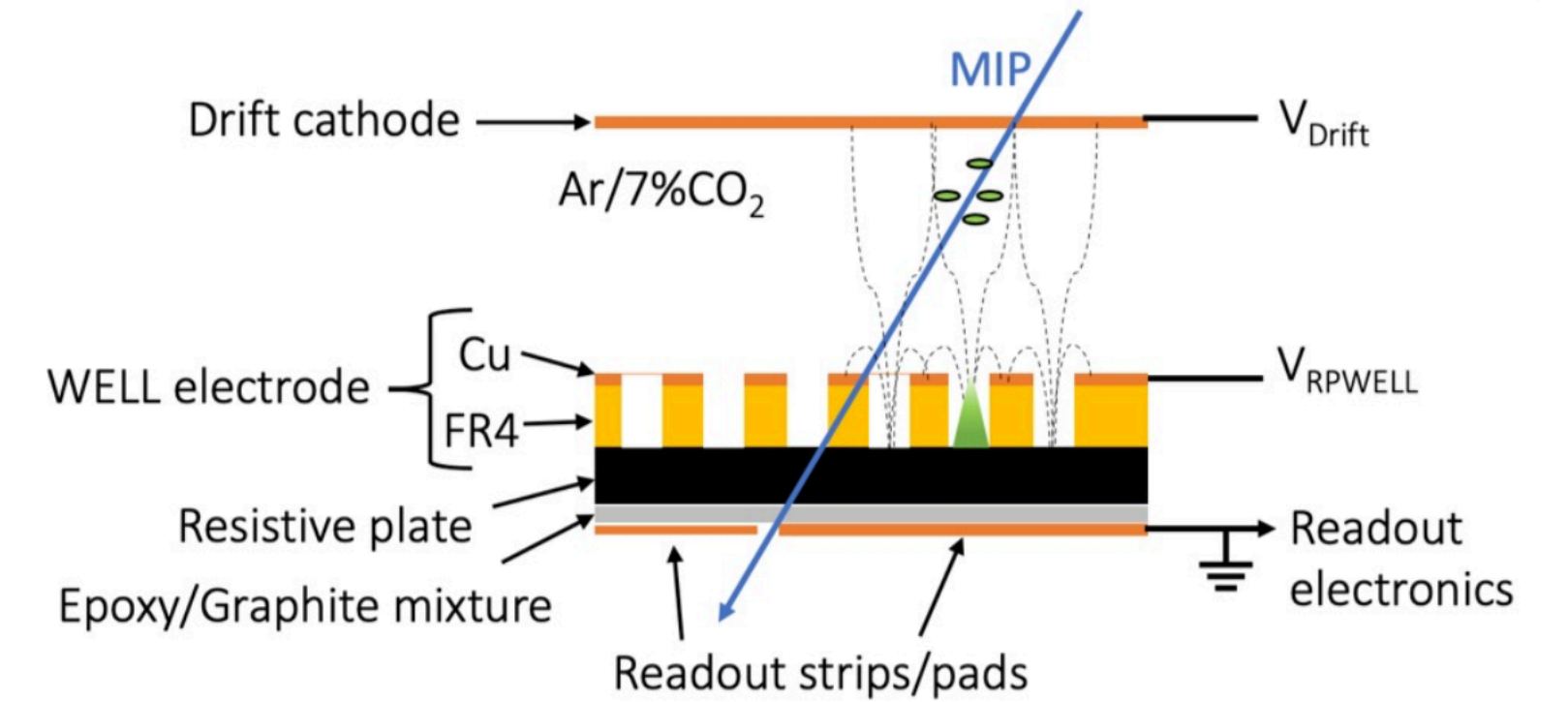
Need 30%/√E

For LC Separate W,Z boson masses on event-by-event basis



- Compact
  - Total volume of 100 m<sup>3</sup> (CEPC TDR)
  - Highly granular -> by using segmented sampling elements:
    - Scintillator tiles – AHCAL
    - Gaseous detectors – (s)DHCAL
- > Available technologies: RPC & MPGDs

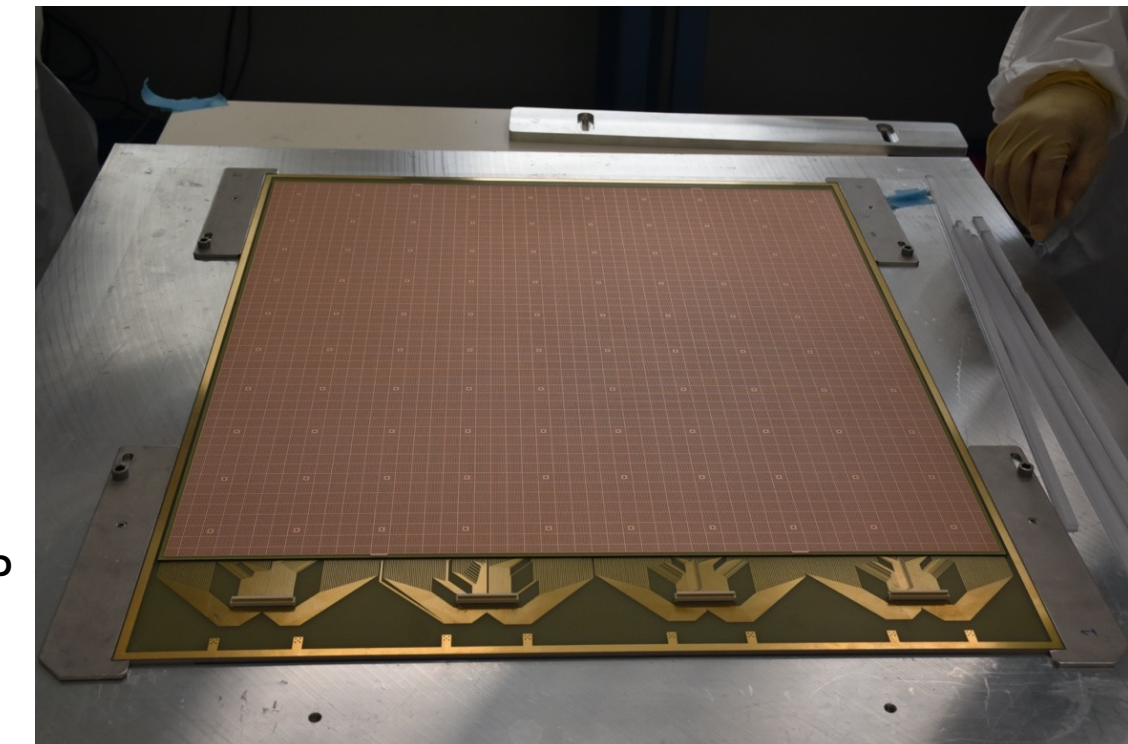
**Combining RPC and MPGD concepts** -> RPWELL: Single-sided Thick GEM electrode coupled to the readout anode through high bulk resistivity



## RPWELL advantages:

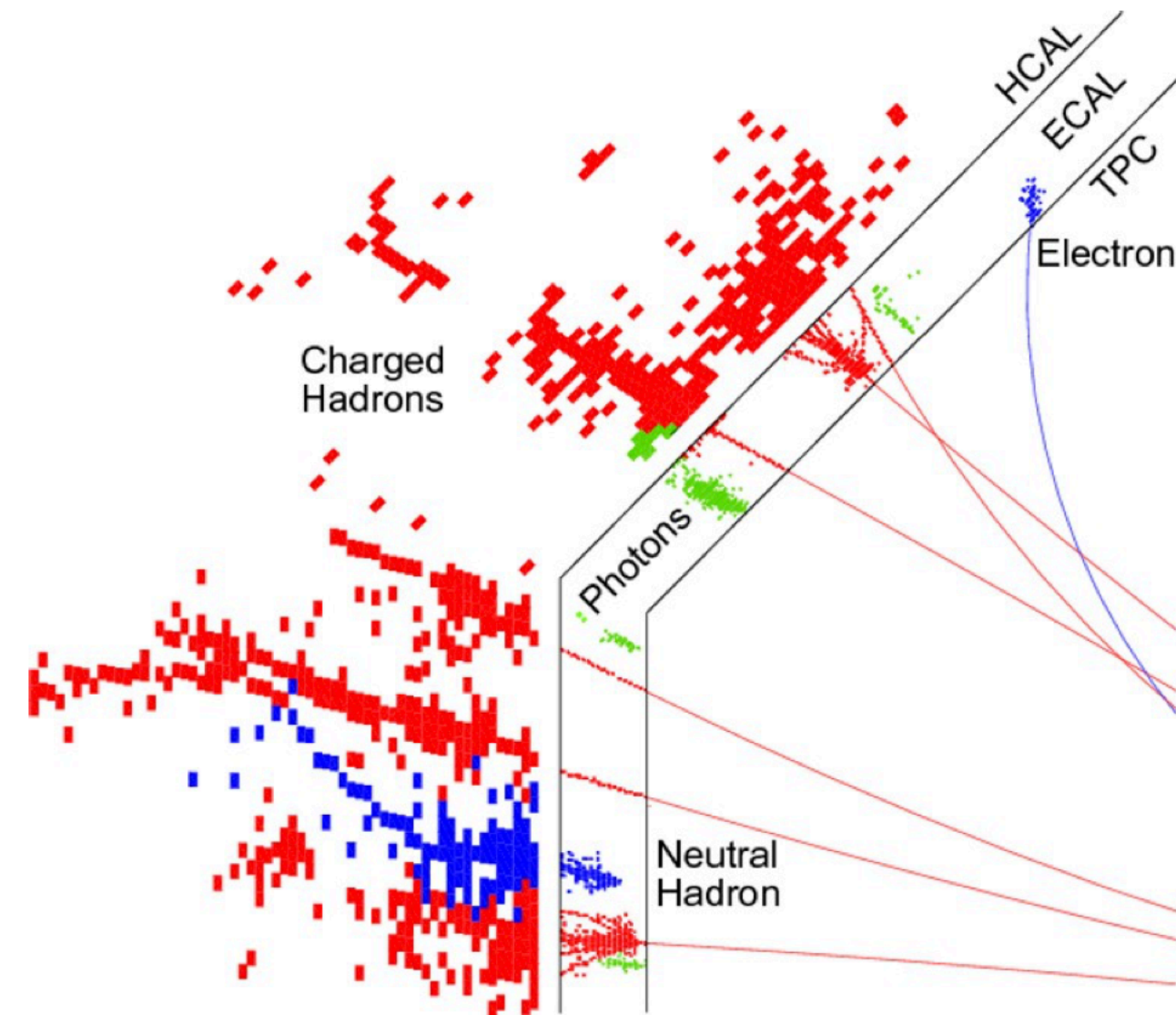
- Operation in environment-friendly gases (Ar)
- Industrially produced
- Robustness
- Simple assembly procedure
- Closed geometry

THGEM on the RP  
50x50 cm<sup>2</sup>



# Digital Hadron Calorimetry: Reconstruction with PFA

Within the ILC community, The **Particle Flow Approach** is considered the most promising strategy for achieving the ILC jet energy resolution goal

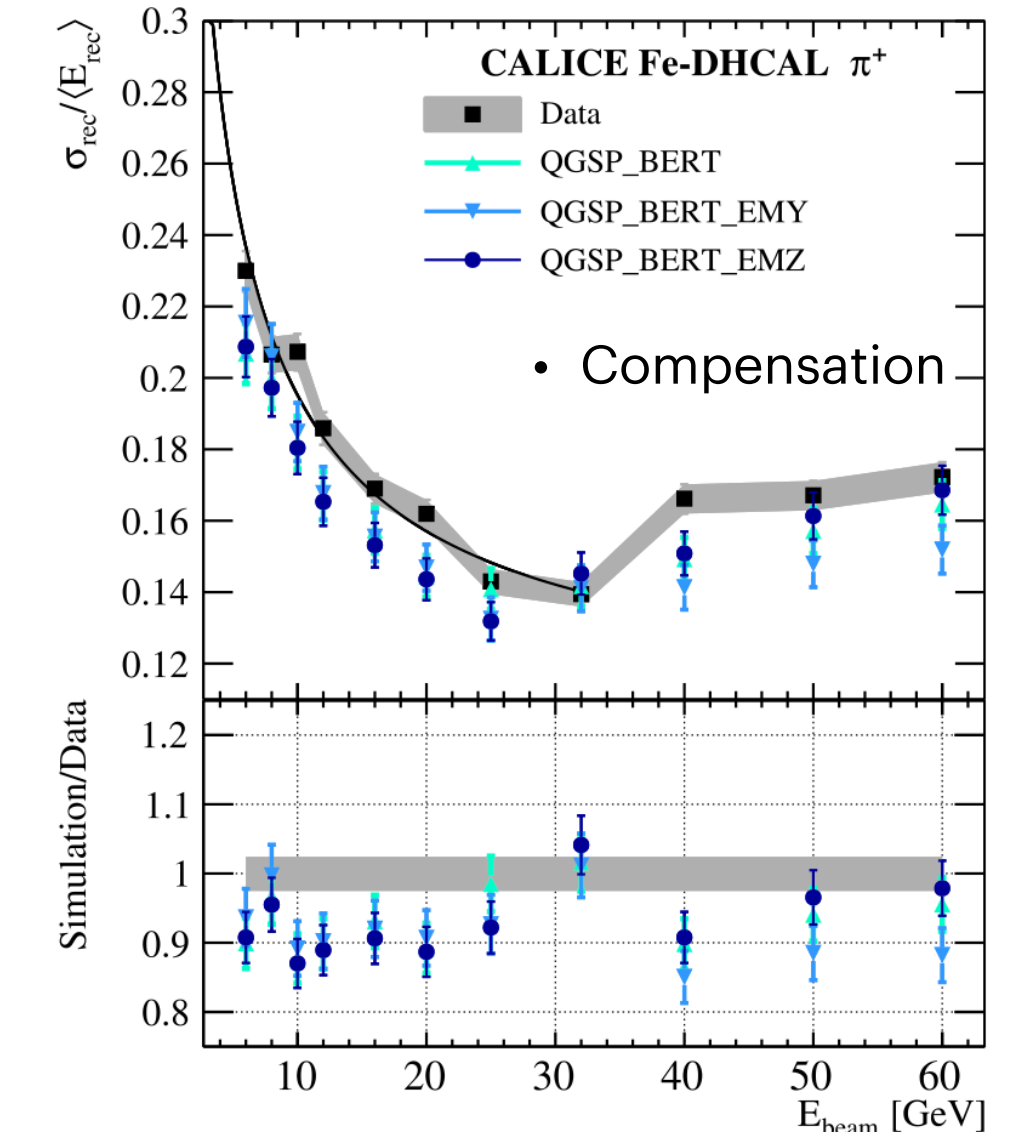
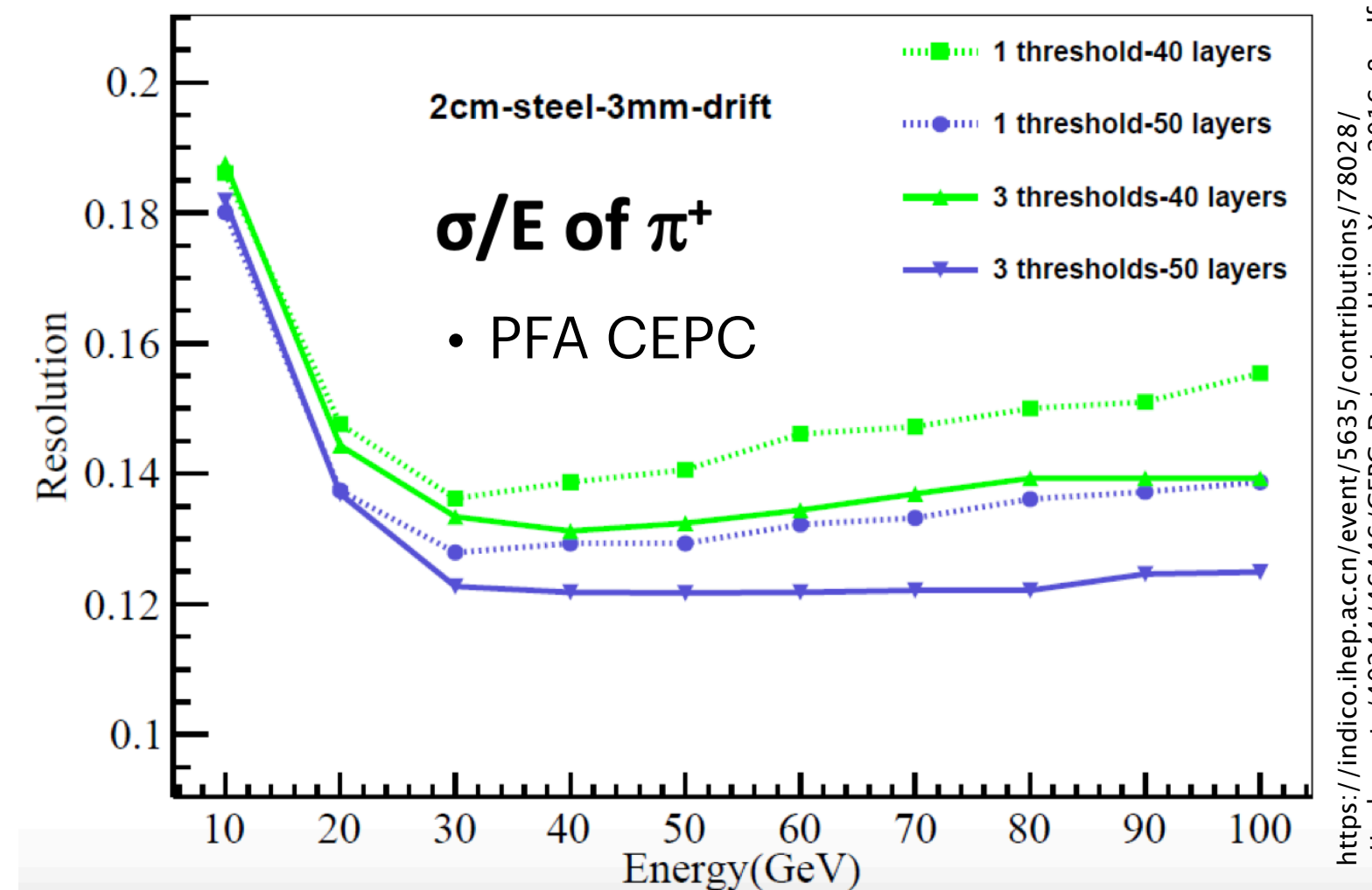


## PFA calorimetry requires:

- The reconstruction of the 4-momentum of all visible particles in an event.
- The momenta of charged particles are measured in the tracking detectors, while the energy measurements for photons and neutral hadrons are obtained from the calorimeters.

With PandoraPFA and ILD simulation obtain:

$E_{JET}$	$\sigma_E/E = \alpha/\sqrt{E_{jj}}$ $ \cos\theta  < 0.7$	$\sigma_E/E_j$
45 GeV	25.2 %	3.7 %
100 GeV	29.2 %	2.9 %
180 GeV	40.3 %	3.0 %
250 GeV	49.3 %	3.1 %



## Drawbacks

- Requires significant processing power.
- Tuning PF algorithms for optimal performance is time-consuming and requires expertise.
- Detector imperfections can impact PF accuracy.
- Struggles with high-energy showers and highly dense particle environments.
- While PF techniques are increasingly used, they might not be readily available for all calorimeter systems.

# Machine Learning Approach

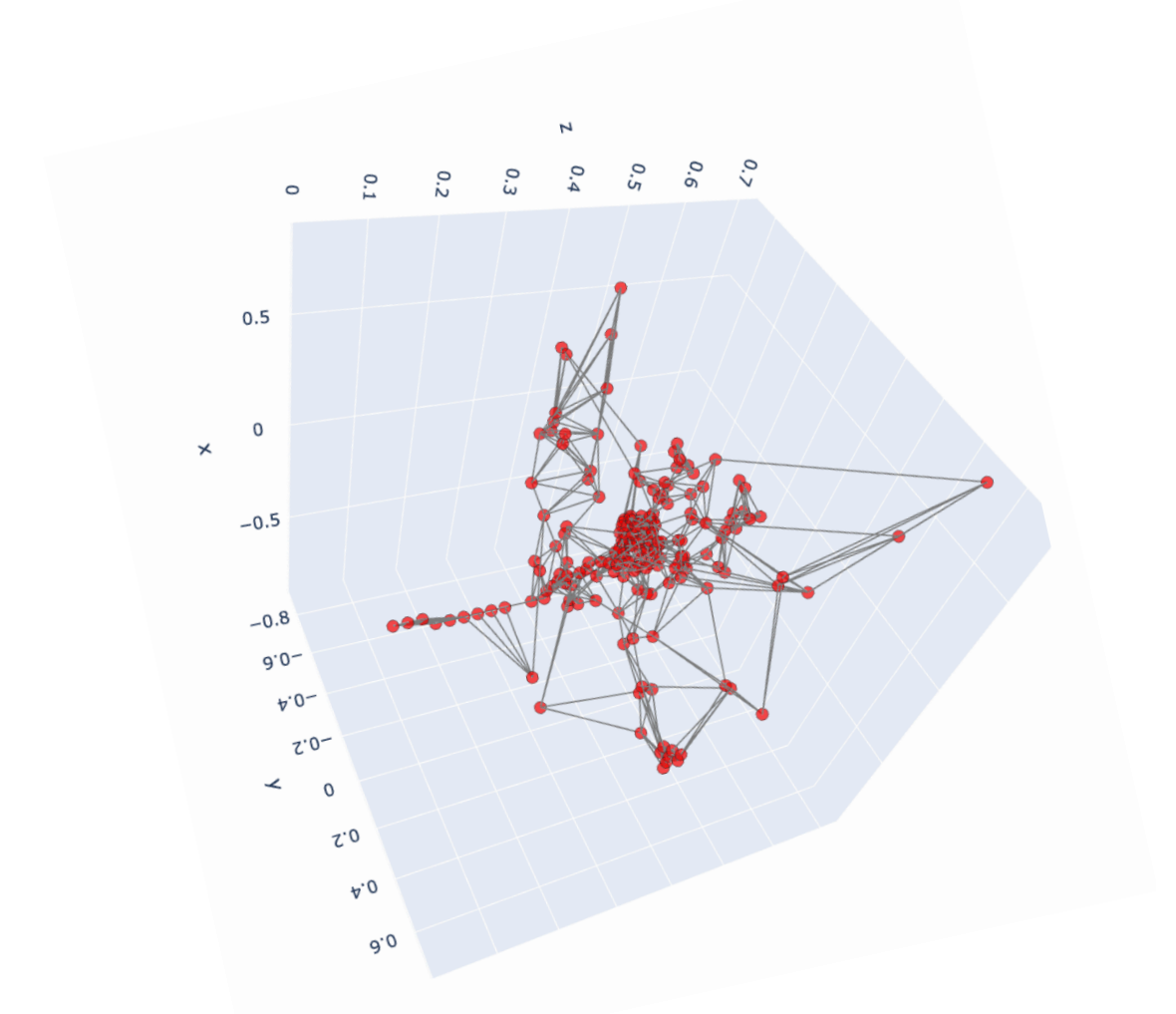
**Graph Neural Networks (GNNs)** have emerged as a powerful tool for problems involving complex relationships between data points.

GNNs offer several advantages when combined with **Deep Sets** or **Graph Attention Networks (GAT)** for shower reconstruction, where particle interactions create intricate shower patterns.

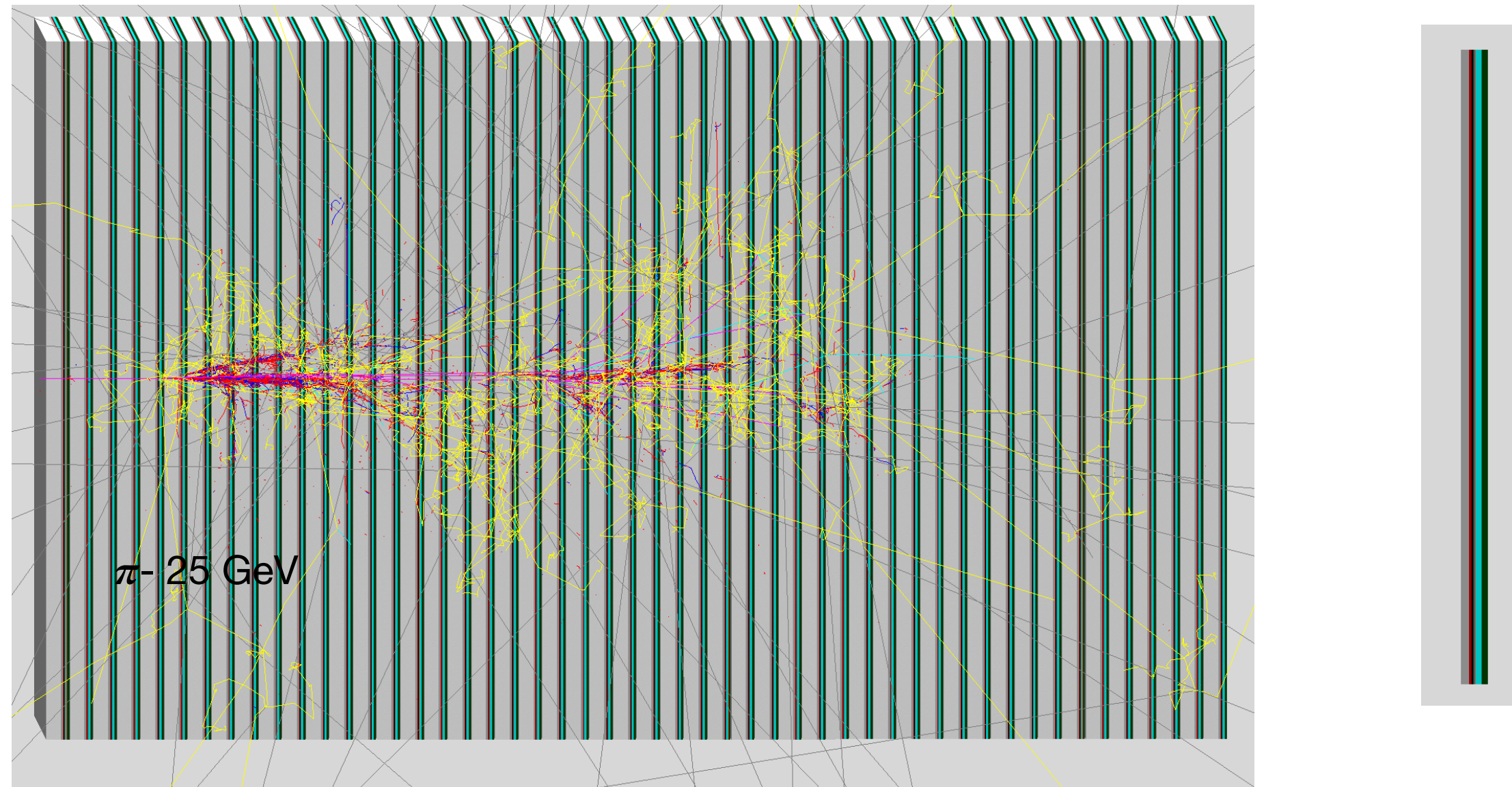
Shower data can be noisy due to detector limitations or background effects. GNNs can potentially learn to identify and down-weight the influence of noisy data.

## GNNs can be applied

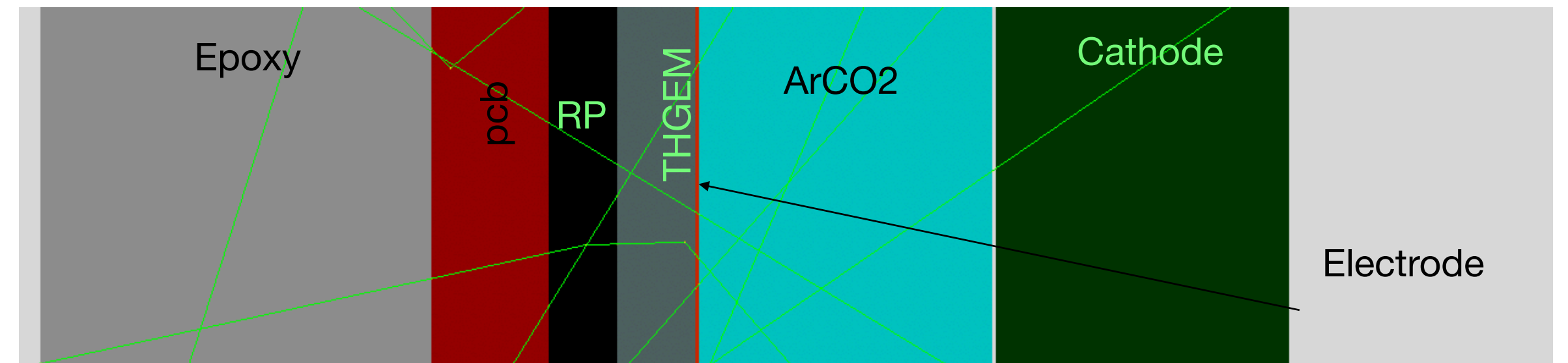
- to the data from complex detector geometries.
- to sparse data with variable input sizes.
- to non-Euclidean data (unlike convolutional neural networks).
- to an end-to-end training framework, where the model learns both feature extraction and shower reconstruction simultaneously.



# 50 layers RPWELL-based DHCAL in Geant4



## Detector module in G4



Resistive Plate WELL detector

G4 v.10.7, QGSP\_BERT\_EMZ  
 10M  $\pi^-$  showers  
 1 to 60GeV  
 $0 < \theta < 40^\circ$ ,  $0 < \phi < 360^\circ$

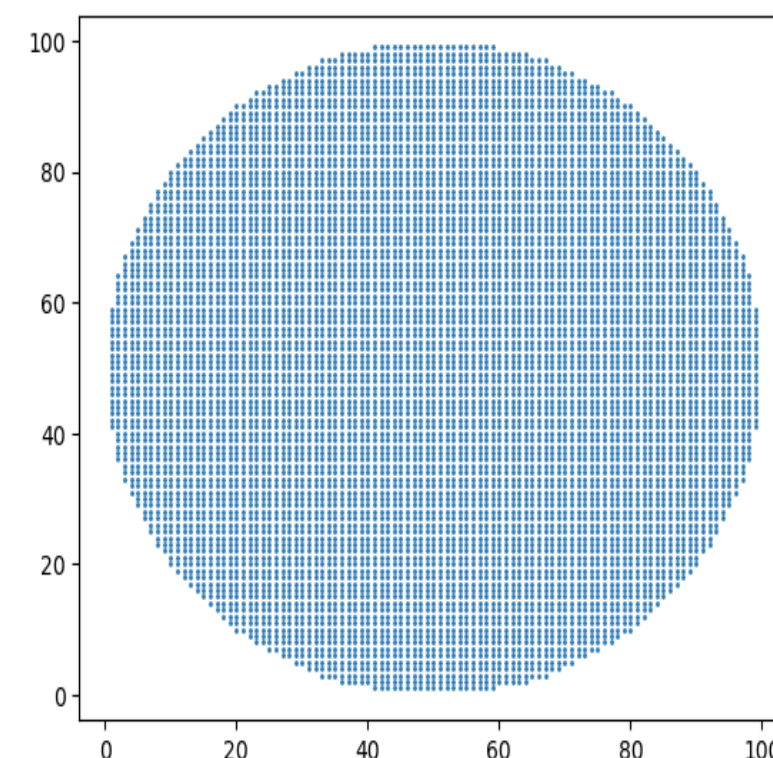
A response of sampling calorimeter to hadrons is much more complicated than to electrons:

- electromagnetic (mostly from  $\pi^0$  particles and nuclear photons)
- hadronic (“invisible” component (neutrons, nuclear binding energy losses, etc.)

The fractional containment of the mentioned components **fluctuates significantly from event to event**

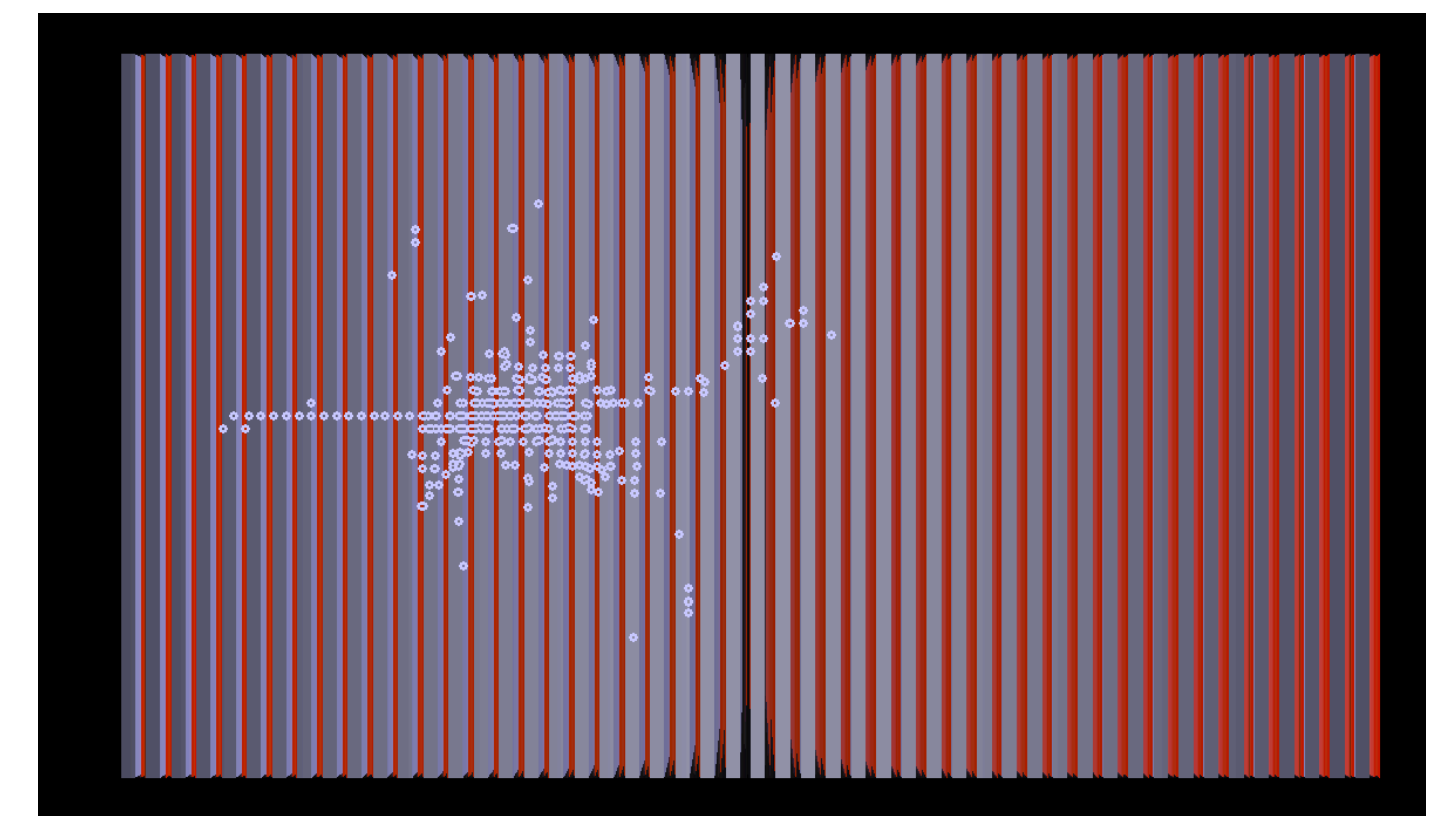
[\*] The simulation was validated against data in a compact module

[\*] D. Shaked-Renous et al., Test-beam and simulation studies towards RPWELL-based DHCAL JINST 17. (2020) P12008.



Digitization Assuming:

- uniform response
- 98% MIP detection efficiency
- 1.1 average pad multiplicity



# DeepSet Architecture

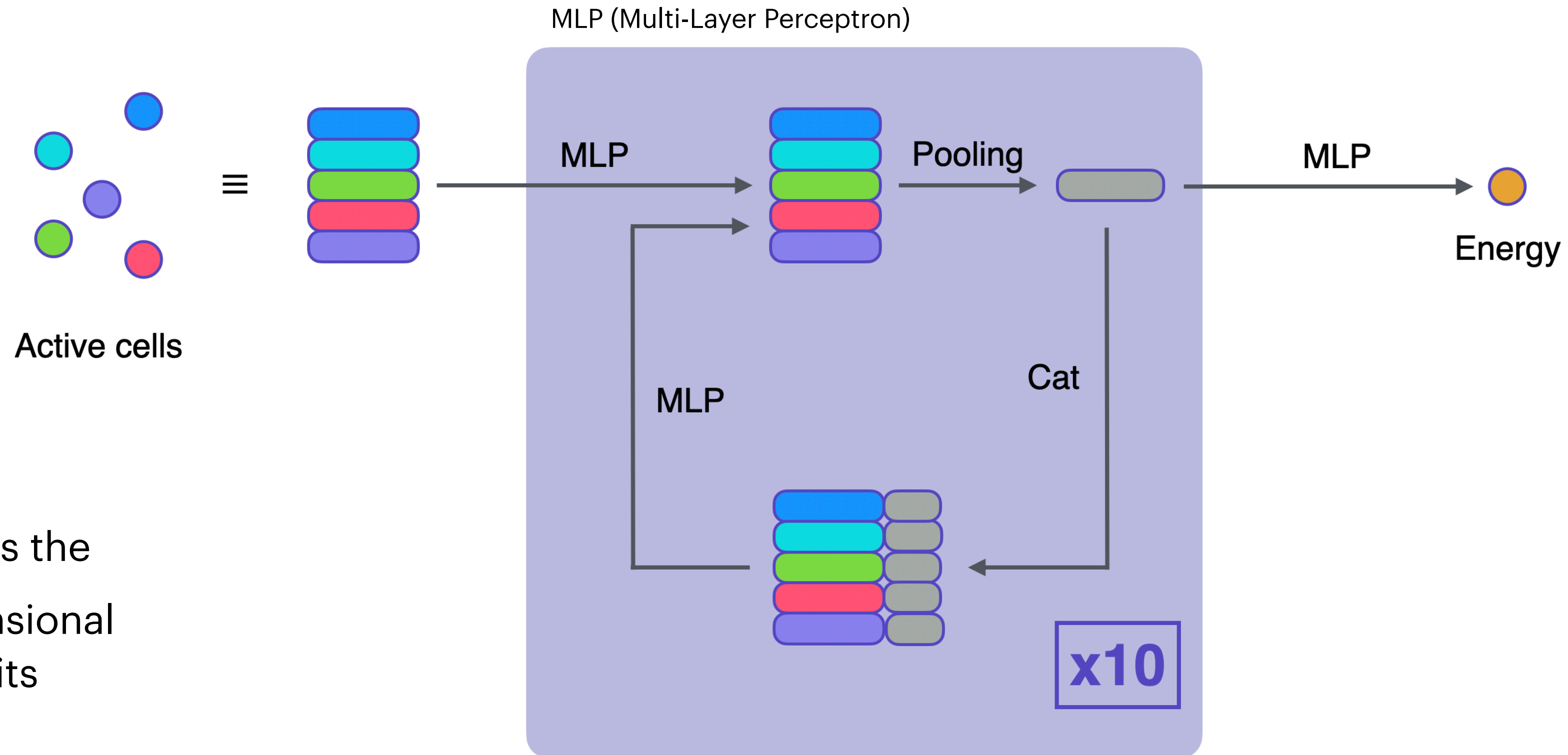
The Deep Set architecture is a powerful approach for dealing with sets of data points, particularly when the order of data points within the set is irrelevant.

⇒ Data structure:

**Point Clouds (PCs)** of  
x, y, z position of hits

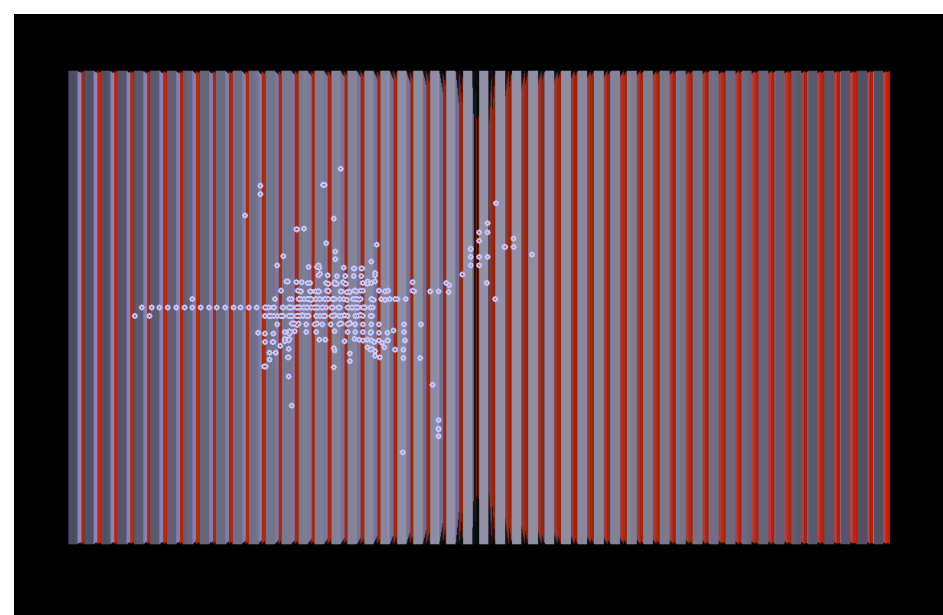
⇒ embedding function transforms the raw data point into a lower-dimensional vector representation, capturing its essential features.

⇒ The core concept of Deep Sets lies in aggregating information from all the element embeddings within the set. This aggregation aims to capture a global representation of the entire set, regardless of the order in which the elements were presented

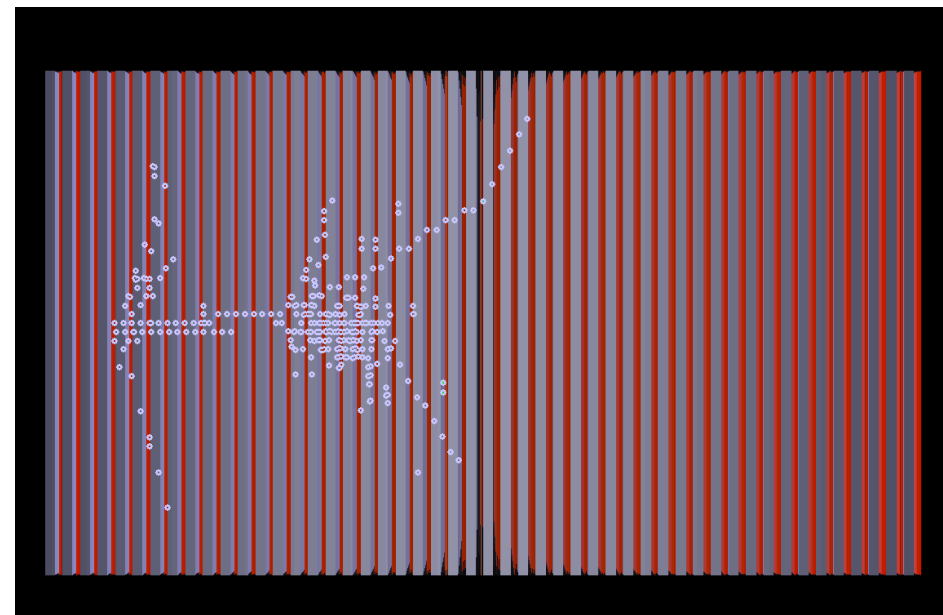


# Data sets

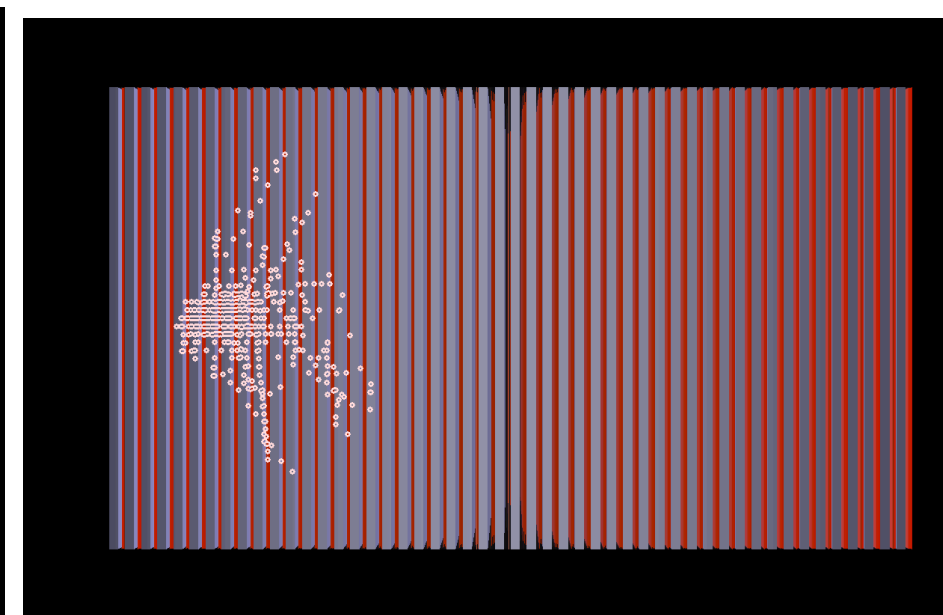
Pions



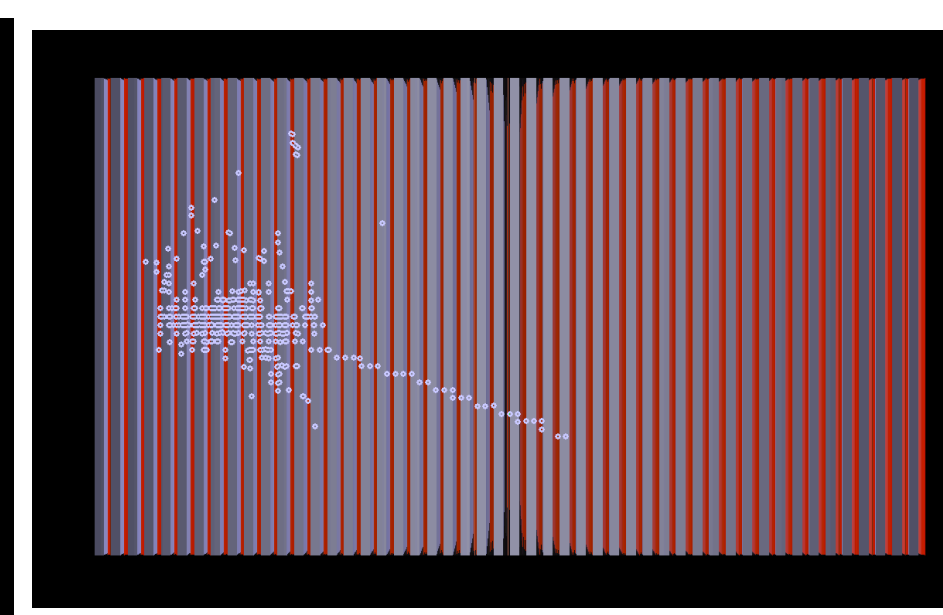
Protons



Neutrons

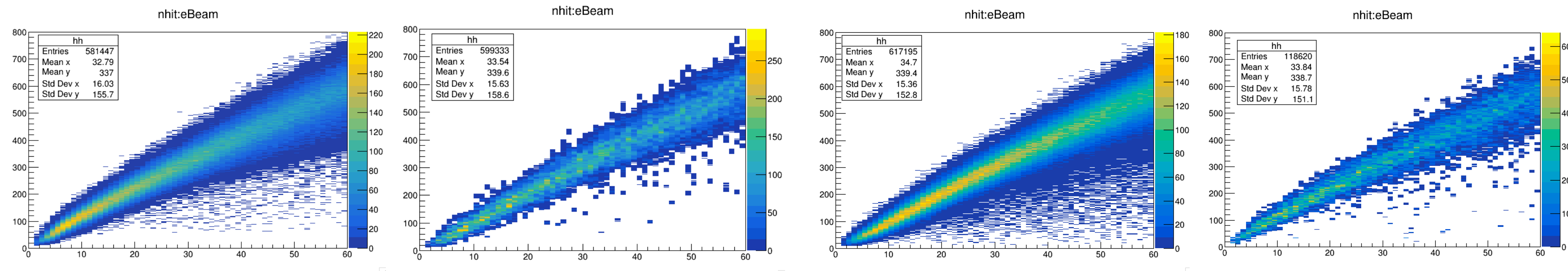


Kaons

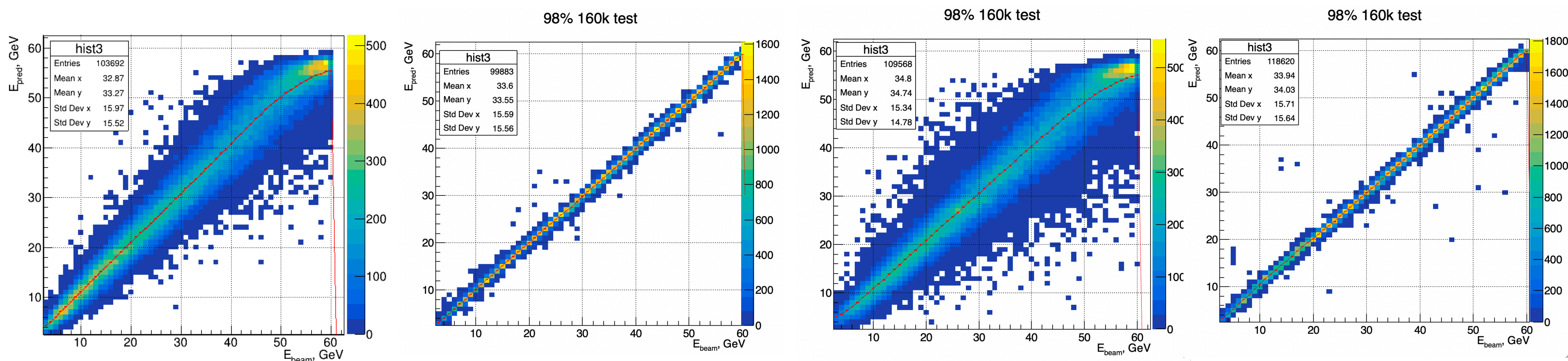


- **training set ~1e6 showers** for 4 different particle types;
- **validation set of 150k showers,**
- **test set- 160k events** for each type

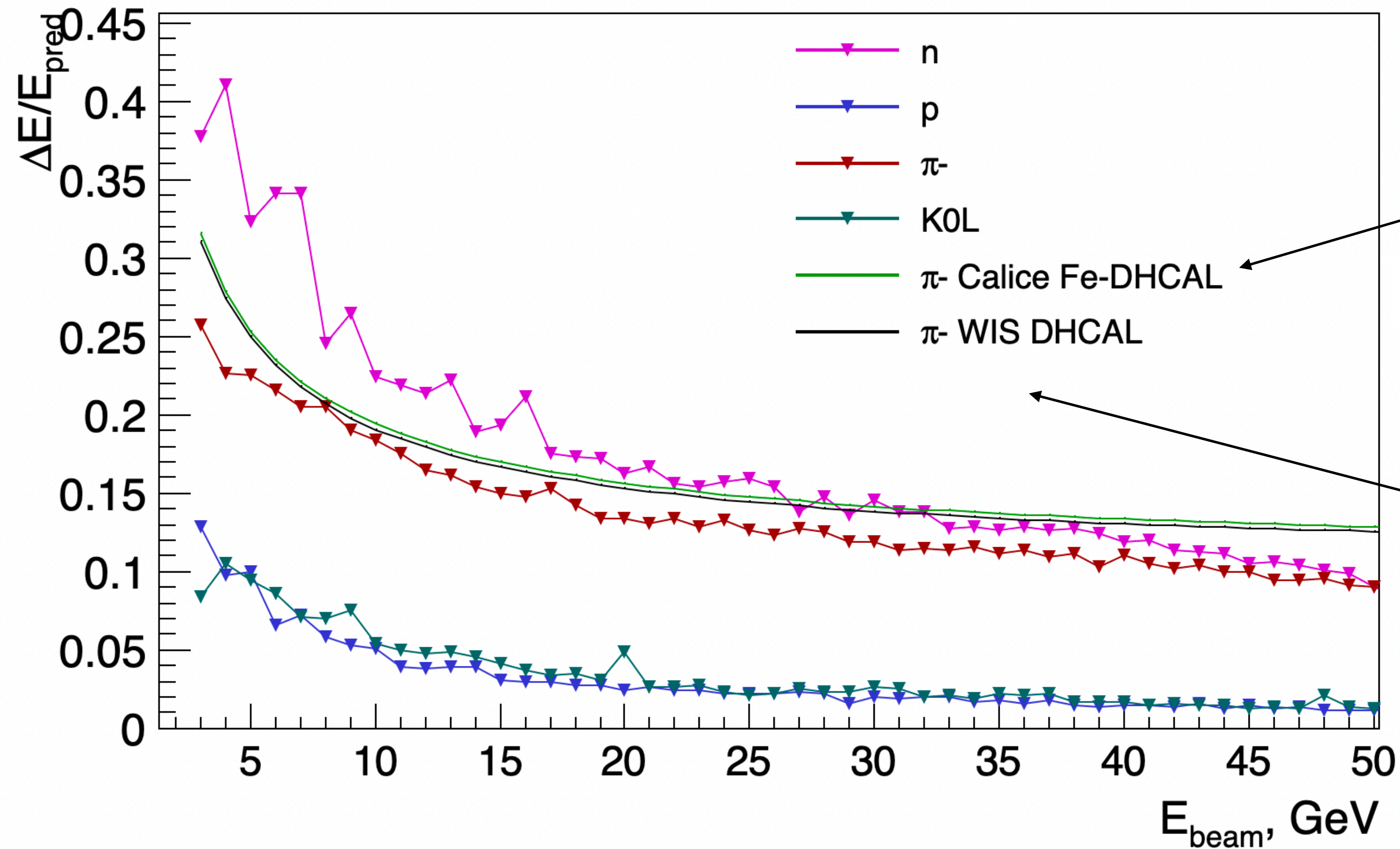
Calorimeter response with the multiplicity of 1:



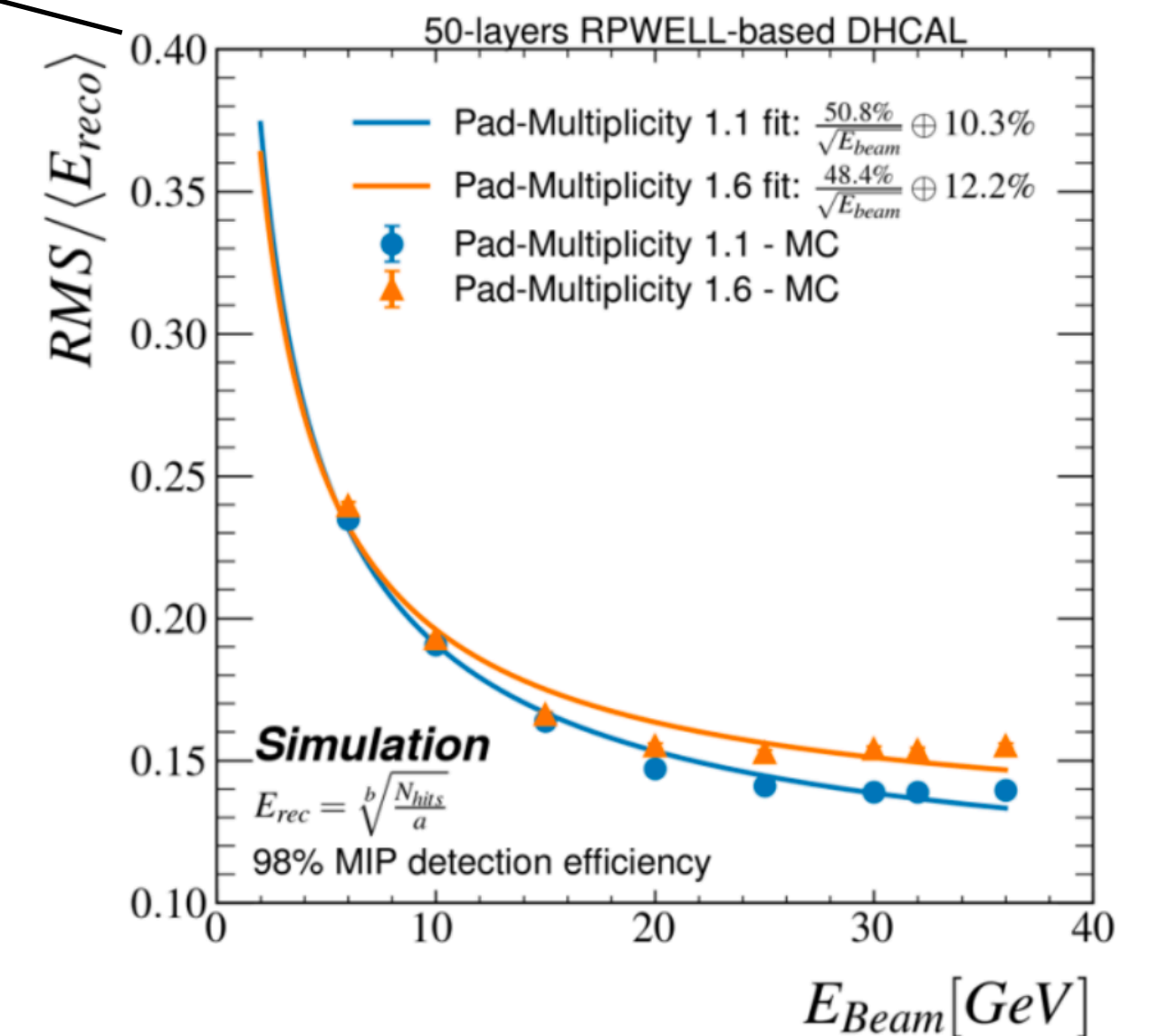
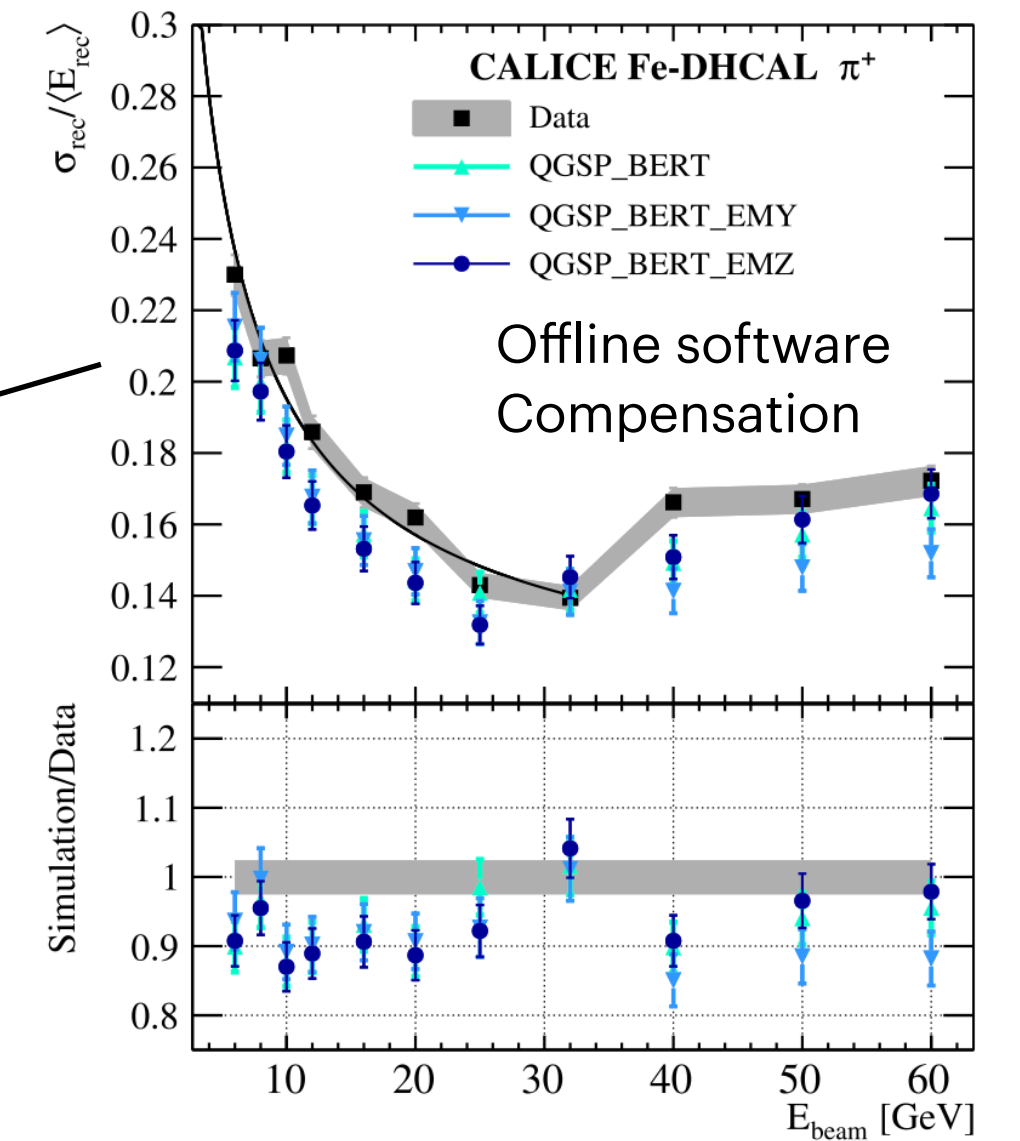
Prediction with DeepSet:



# Energy resolution predictions with DeepSet



$$\frac{\sigma}{E} = \frac{a}{\sqrt{E}} \oplus b$$



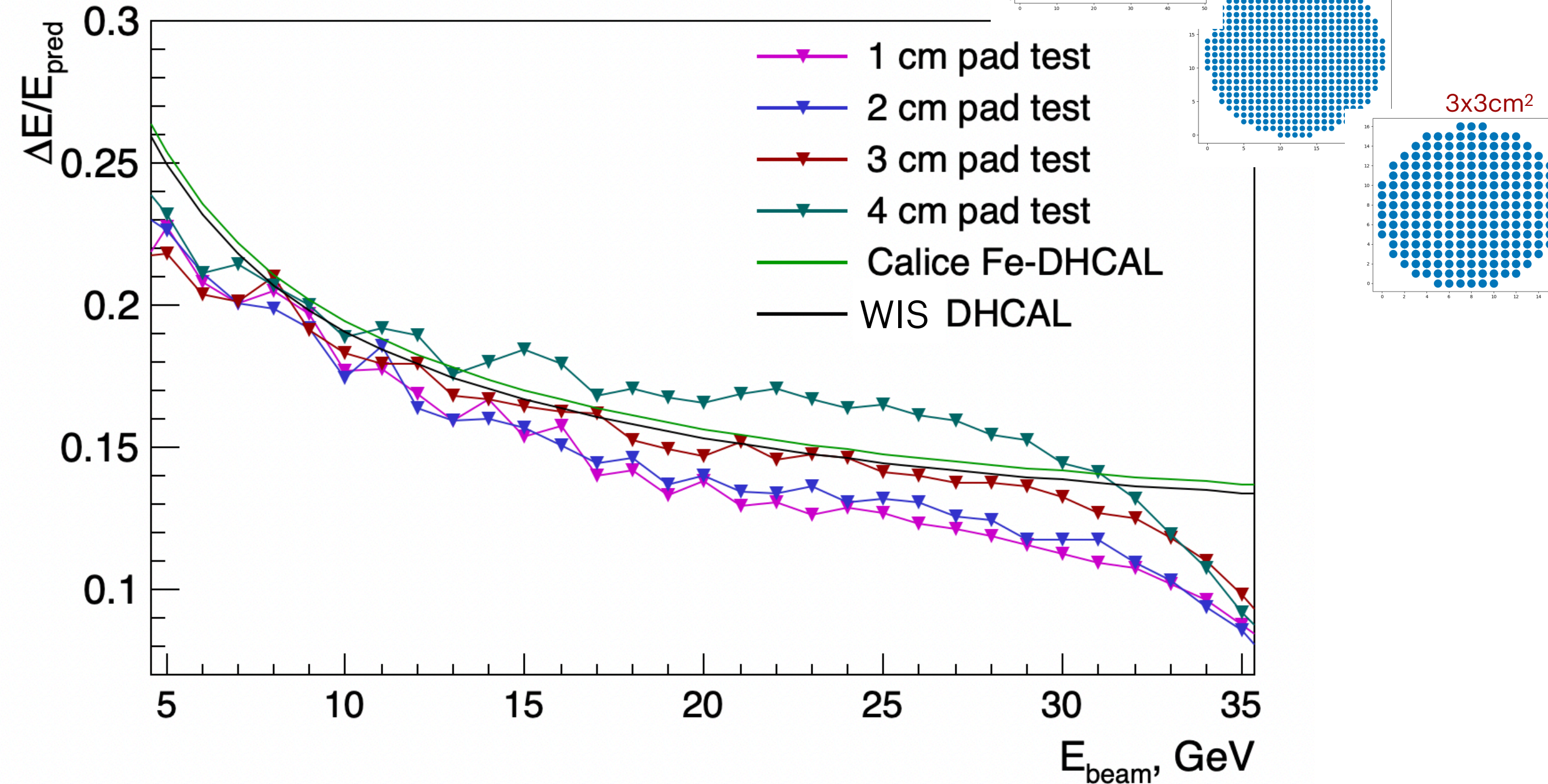
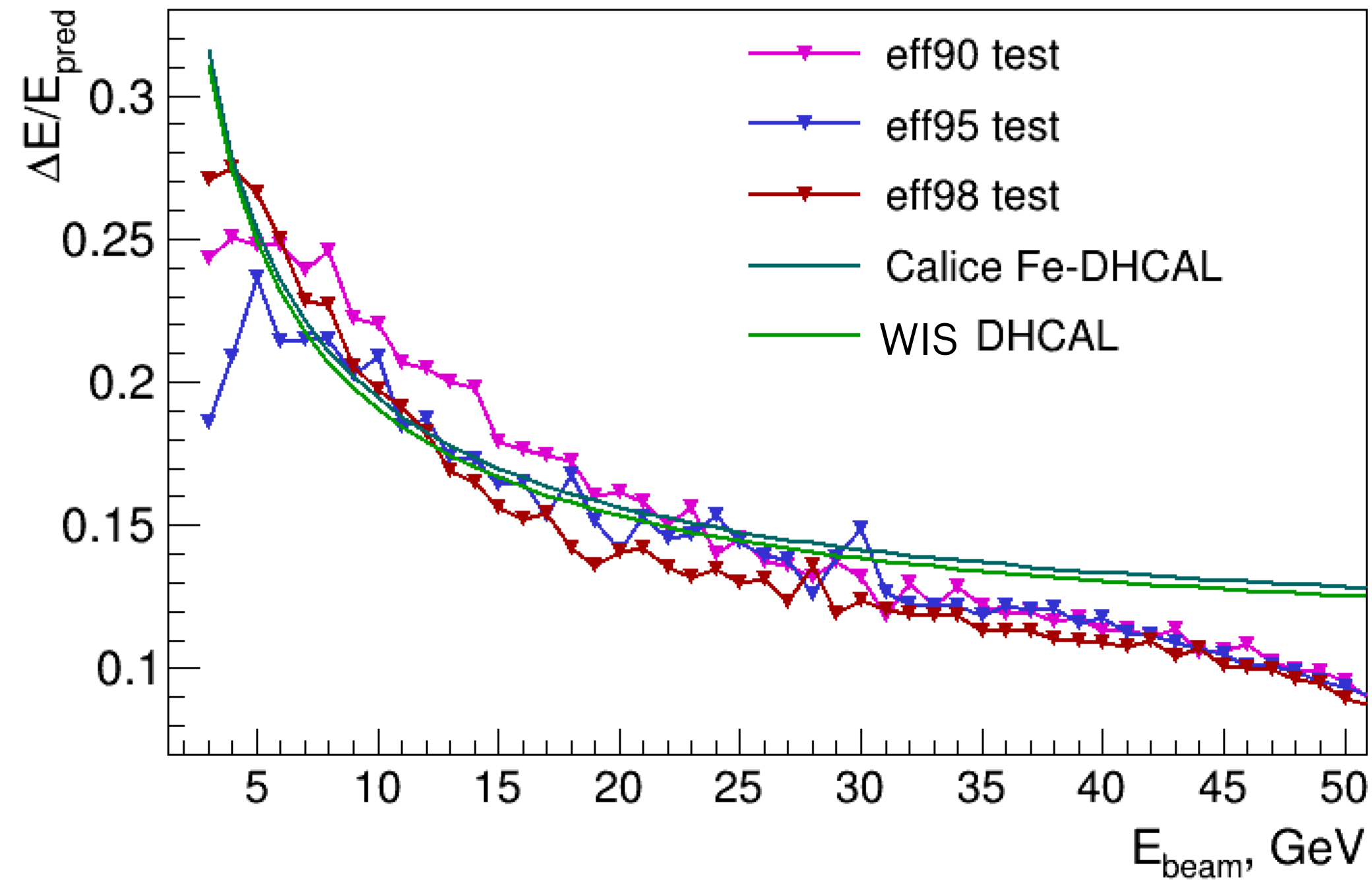
● The energy resolution measured for pions (red line) **outperforms rule-based algorithms** for the RPWELL-based WIS DHCAL [\*] (black line) and RPC-based CALICE DHCAL [\*\*] (green line)

[\*] D. Shaked-Renous et al., Test-beam and simulation studies towards RPWELL-based DHCAL JINST 17. (2020) P12008.

[\*\*] CALICE Collaboration, Analysis of Testbeam Data of the Highly Granular RPC-Steel CALICE Digital Hadron Calorimeter and Validation of Geant4 Monte Carlo Model, NIM A 939. (2019) 89–105

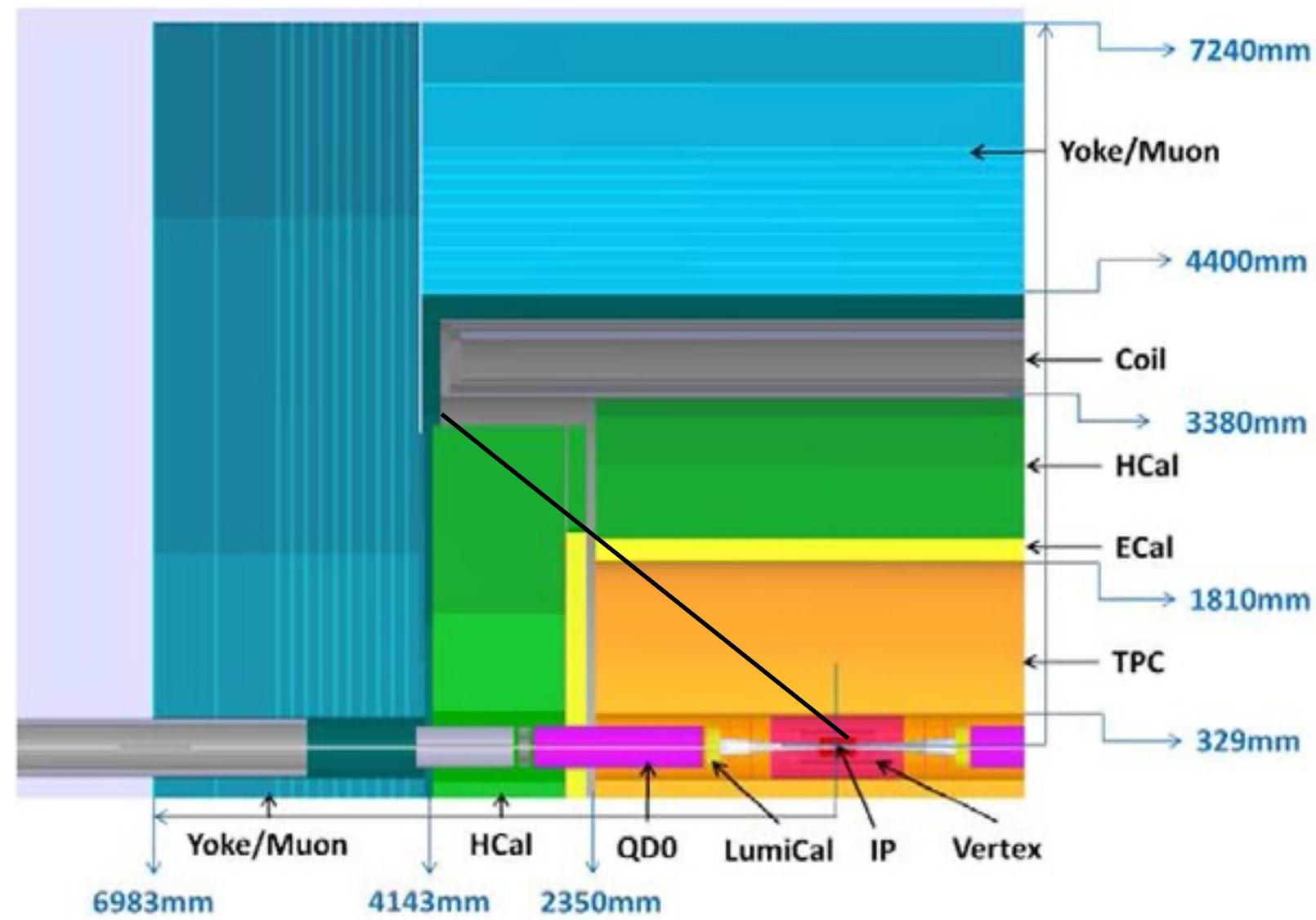


# Predictions for pions with different pad sizes and efficiencies

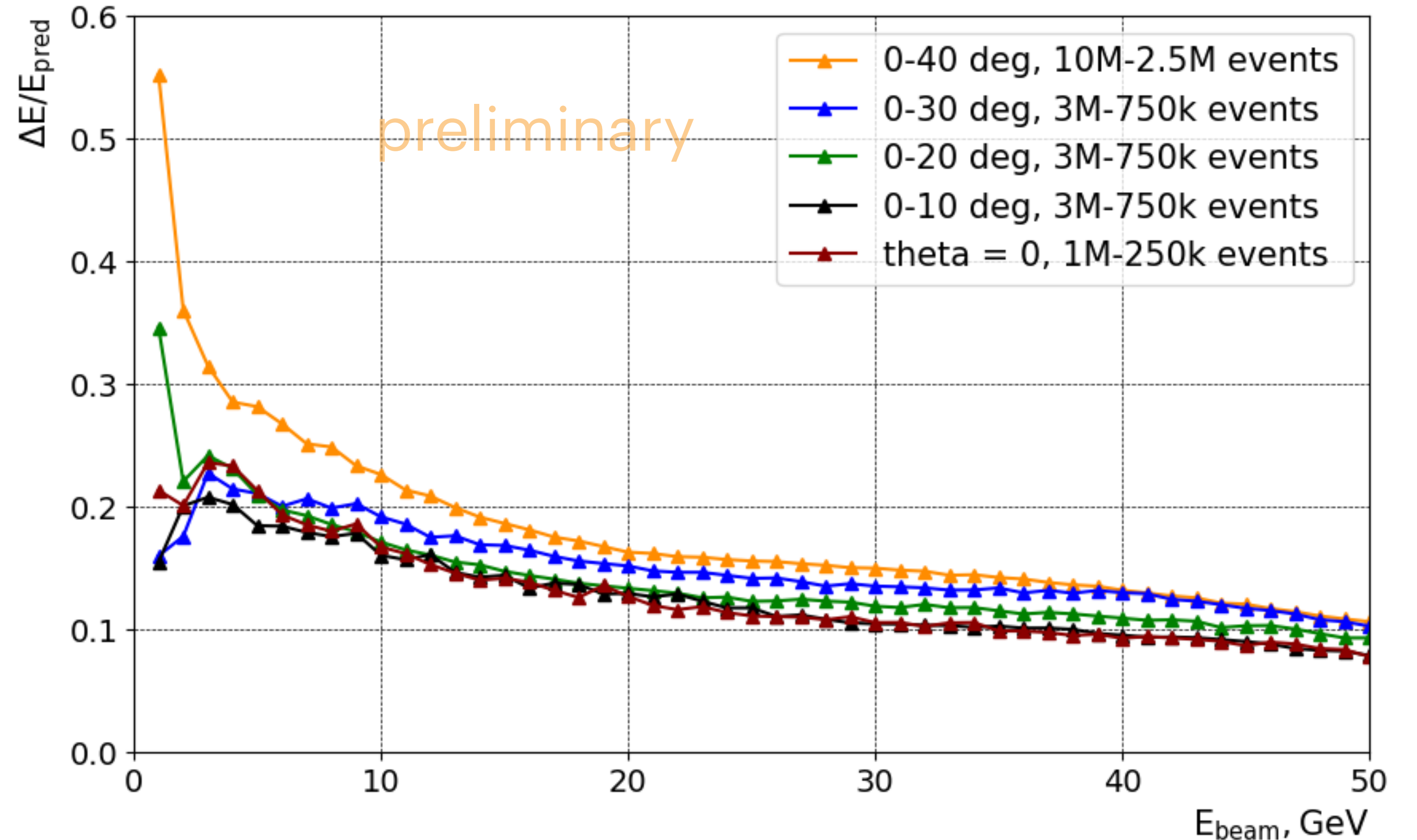


- Enlarging the pads by a factor of four ( $s \times \text{cm}^2$ ) and reducing the number of channels by four does not degrade the performance significantly.
- Provided that the two shower separations would not degrade as well, these may offer a more cost-effective solution for future experiments.
- The results are consistent above 30 GeV for all studied MIP detection efficiencies but degrade significantly at lower energies at 90% MIP detection efficiency.

# Predictions for pions with different shower angles

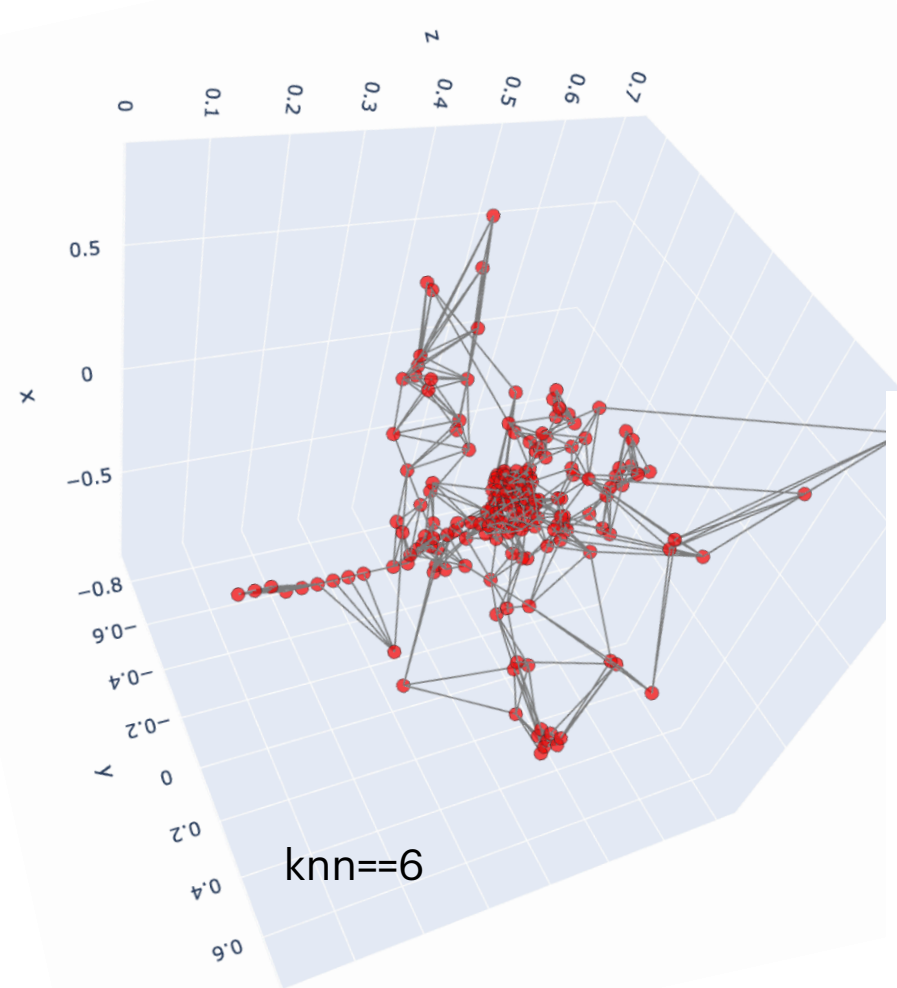


The structure of the baseline CEPC detector design

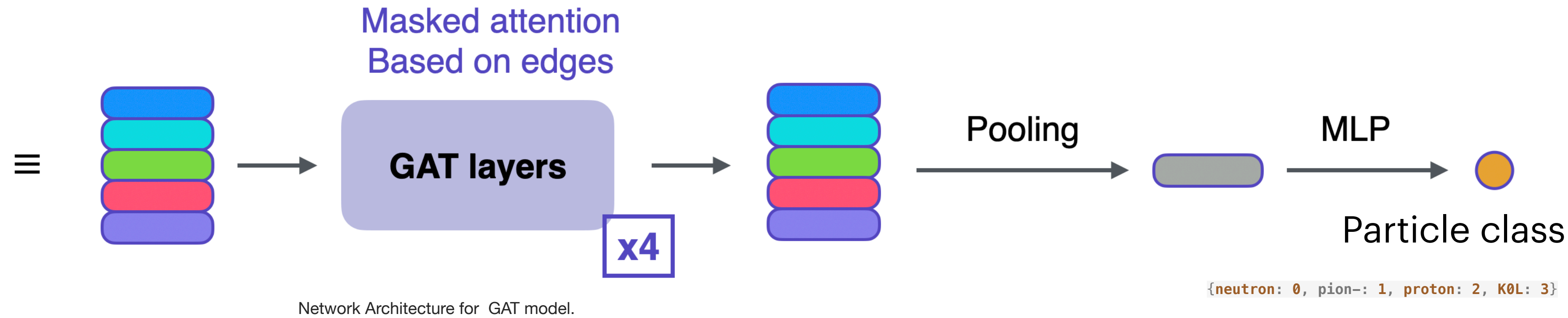
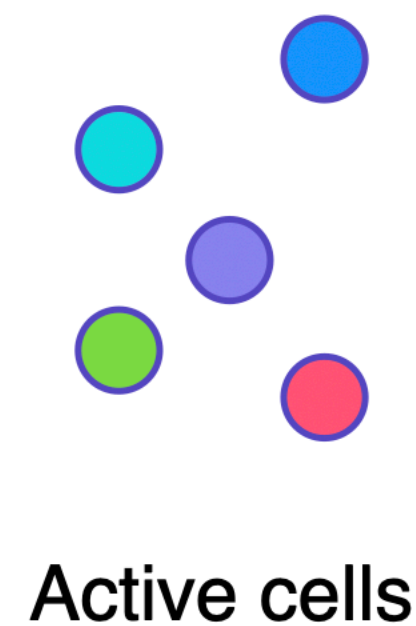


- Good prediction ability for the polar angle uniformly distributed in the range of 0 - 20° ;
- adding angles > 20° degrades the performance
- Ongoing training on 10e6 data set for the polar angle range of 0 - 40°.

# GAT for classification



The **k-nearest neighbor graph (k-NNG)** is a graph in which two vertices  $p$  and  $q$  are connected by an edge, if the distance between  $p$  and  $q$  is among the  $k$ -th smallest distances from  $p$  to other objects from  $P$ .

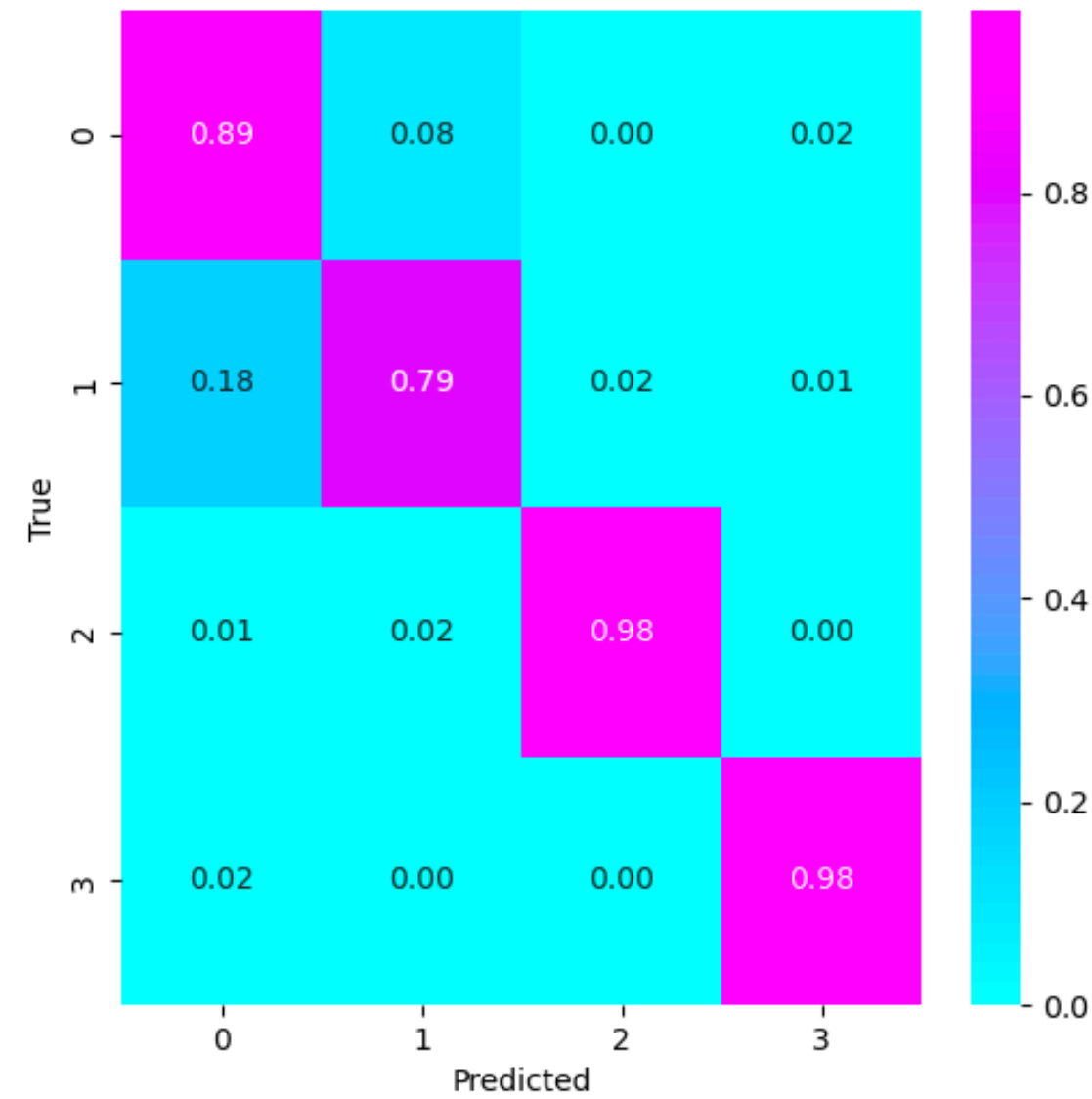


- Graph attention transformers (GAT) - novel convolution-style NN that operate on graph-structured data, leveraging masked self-attentional layers.
- Unlike Deep Sets for point clouds, this approach leverages **edges** in addition to nodes. This allows the Graph Attention Network (GAT) layers to exploit the inherent **structural information** within the shower data
- We employ a **masked attention** mechanism. This restricts information sharing between nodes to only **geometrically close neighbors**. This focus on local interactions is particularly beneficial for understanding the **shower's shape**.
- While current results are promising, exploring a model variant with **unrestricted attention** (all nodes communicate) is a potential future direction.

# Classification

- the training set ~4e6 showers with 4 different particle types and validation set of 600k showers, each type - 150k events; for all with multiplicity = 1

Confusion matrix



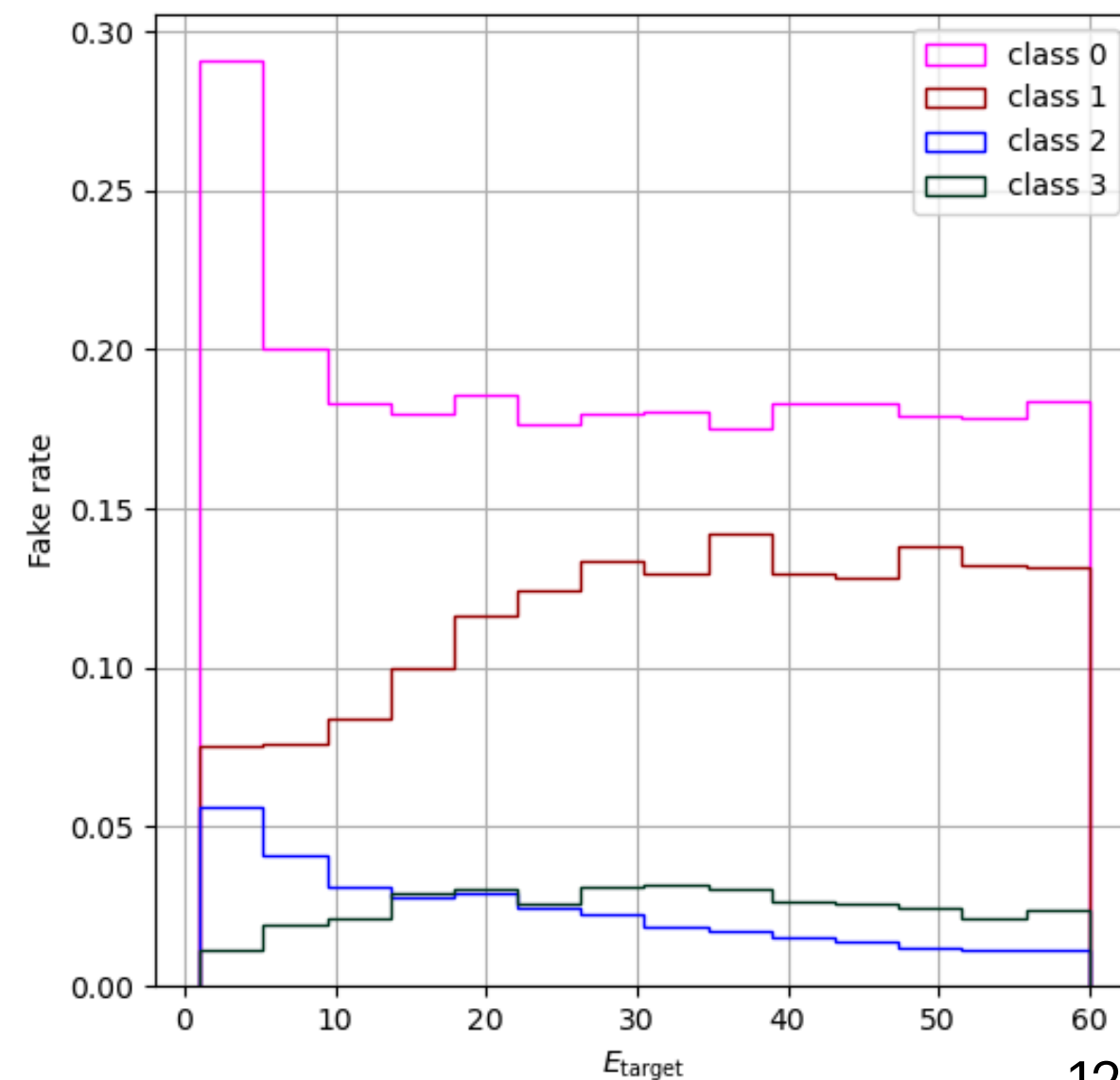
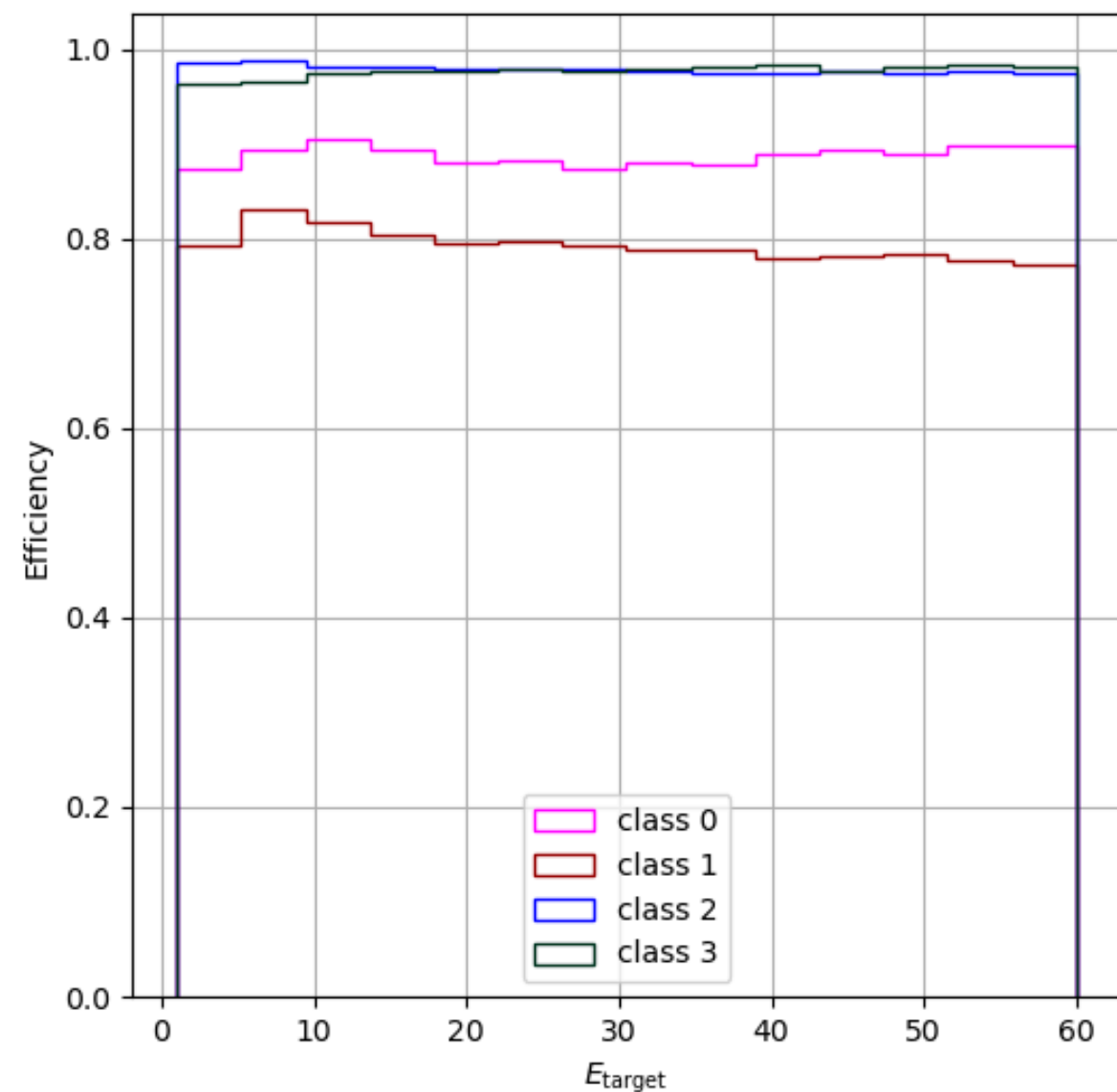
	True k0L	True p	True pi-	True n
k0L	97.91%	0.00%	0.64%	2.23%
p	0.00%	97.86%	1.76%	0.50%
pi-	0.25%	1.57%	79.22%	8.37%
n	1.84%	0.54%	16.02%	89.12%

## Efficiency and fake rate

**Efficiency** (also known as precision or recall) represents the proportion of predicted Class A that are actually Class A.

**Fake rate** represents the proportion of actual negatives (not Class A) that are incorrectly classified as Class A

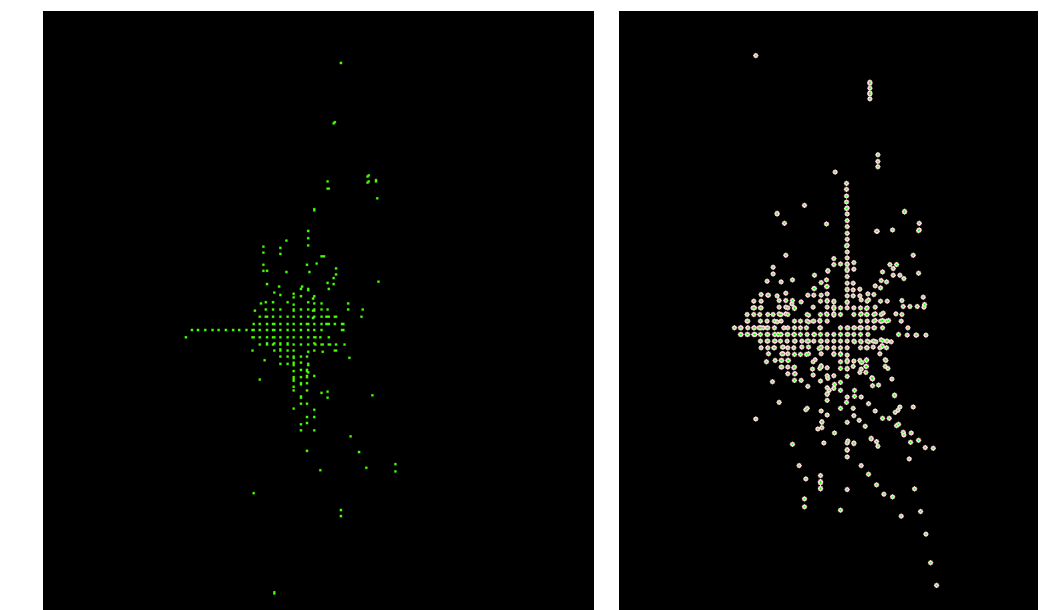
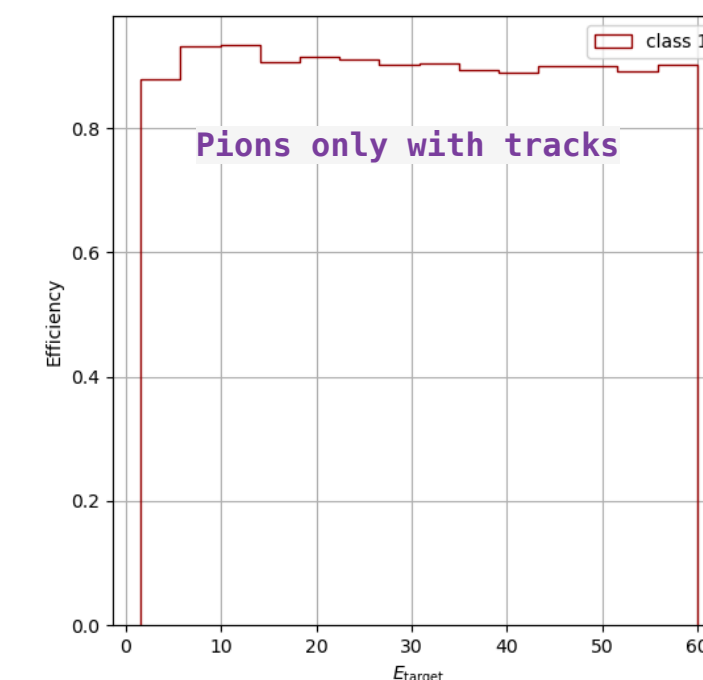
Class = {neutron: 0, pion-: 1, proton: 2, K0L: 3}



- Protons and kaons are never misidentified

*"The production of  $\pi^0$ 's in kaon showers is therefore limited by a mechanism very similar to that in proton showers, and the results may be expected to be similar as well"* N. Akchurin et al. NIM. in Phys. Res. A 408 (1998) 380–396

- The best performance is for k0L&p & the worst performance is for pi-



# Outlook

- The energy resolution measured for pions in DHCAL outperforms rule-based algorithms.
  - Enlarging the pads by a factor of four ( $s \times \text{cm}^2$ ) and reducing the number of channels by four does not degrade the performance significantly;
  - The results are consistent above 30 GeV for all studied MIP detection efficiencies but degrade significantly at 90% MIP detection efficiency at lower energies;
  - Good prediction ability for the polar angle uniformly distributed in the range of 0 - 20°;
- Shower discrimination performs very well for protons and kaons and requires additional studies for pions and neutrons.
- Deep learning techniques are emerging as a promising approach to improve hadronic shower and jet energy reconstruction. They are, therefore, an important step towards optimizing DHCAL performance in terms of single hadron and jet energy resolution, two-particle separation, etc.

**Thank you!**

# Back up

# on differences observed in the calorimetric signals generated by protons and pions of the same energies

N. Akchurin et al./Nucl. Instr. and Meth. in Phys. Res. A 408 (1998) 380—396

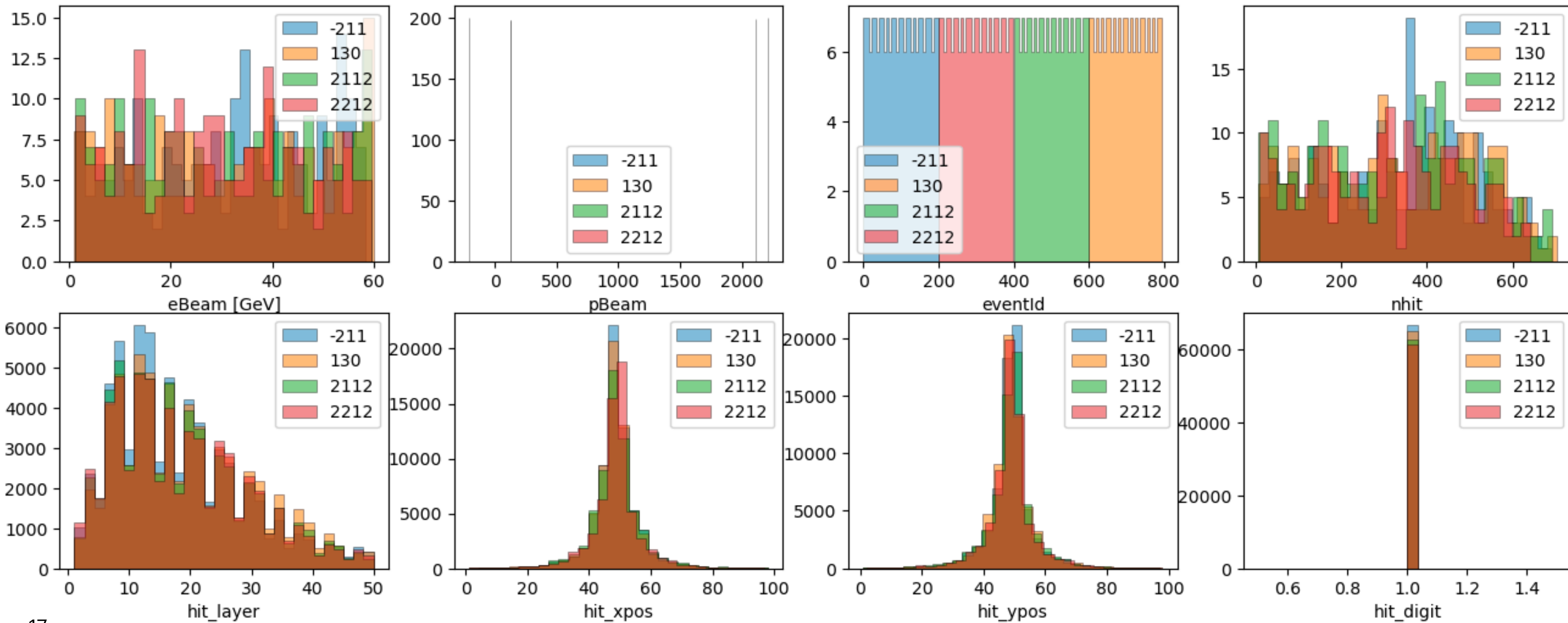
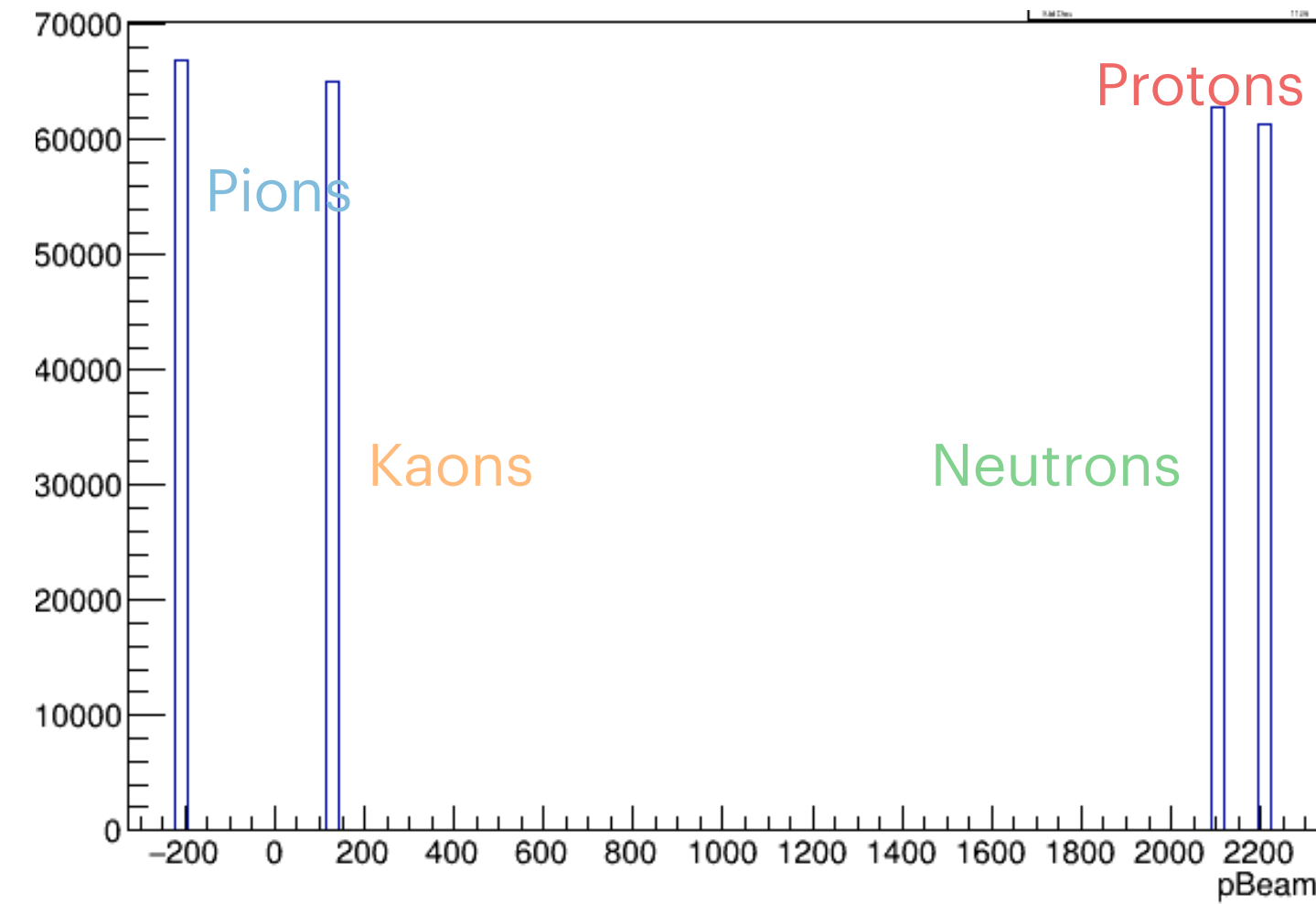
## 5.3. Consequences

The origin of the observed differences between proton and pion showers strongly suggests that the measurable effects are not limited to these particles. In particular, **we expect to see significant differences between kaon and pion showers as well. Just as the baryon number is conserved in proton showers, the strangeness quantum number is conserved in the strong interactions that take place in kaon-induced showers.** The strange (anti-)quark contained in the incident particle is likely to be transferred to a highly energetic particle in each generation of the shower development.

**The production of  $\pi^0$ 's in kaon showers is therefore limited by a mechanism very similar to that in proton showers,** and the results may be expected to be similar as well: a smaller response, a better resolution, a wider shower profile, and a more symmetric line shape than for pion-induced showers.



# G4 sample for shower discrimination studies



# 850:90 - 8 Net Layers GAT8L vs 2M:160k DS 10L

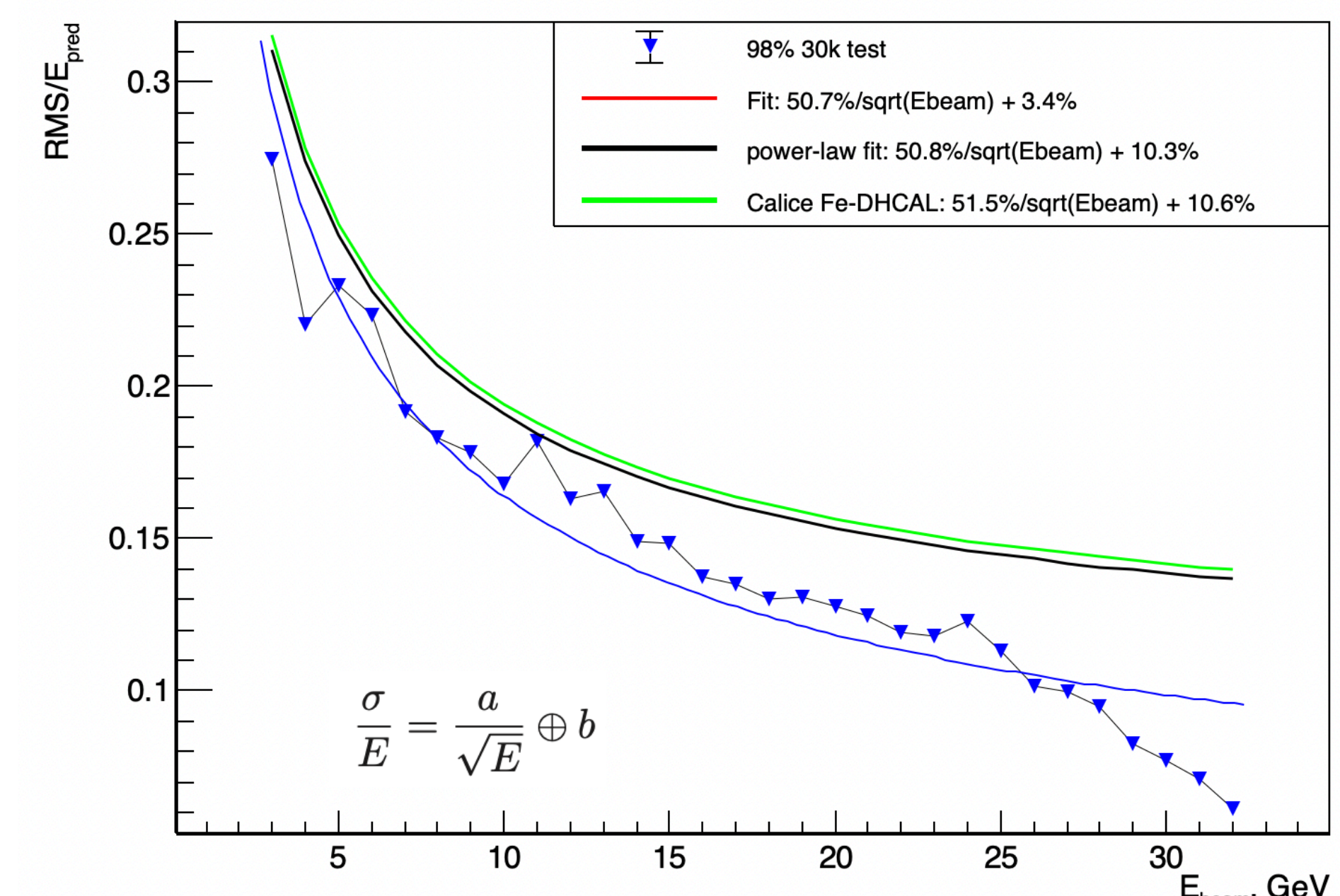
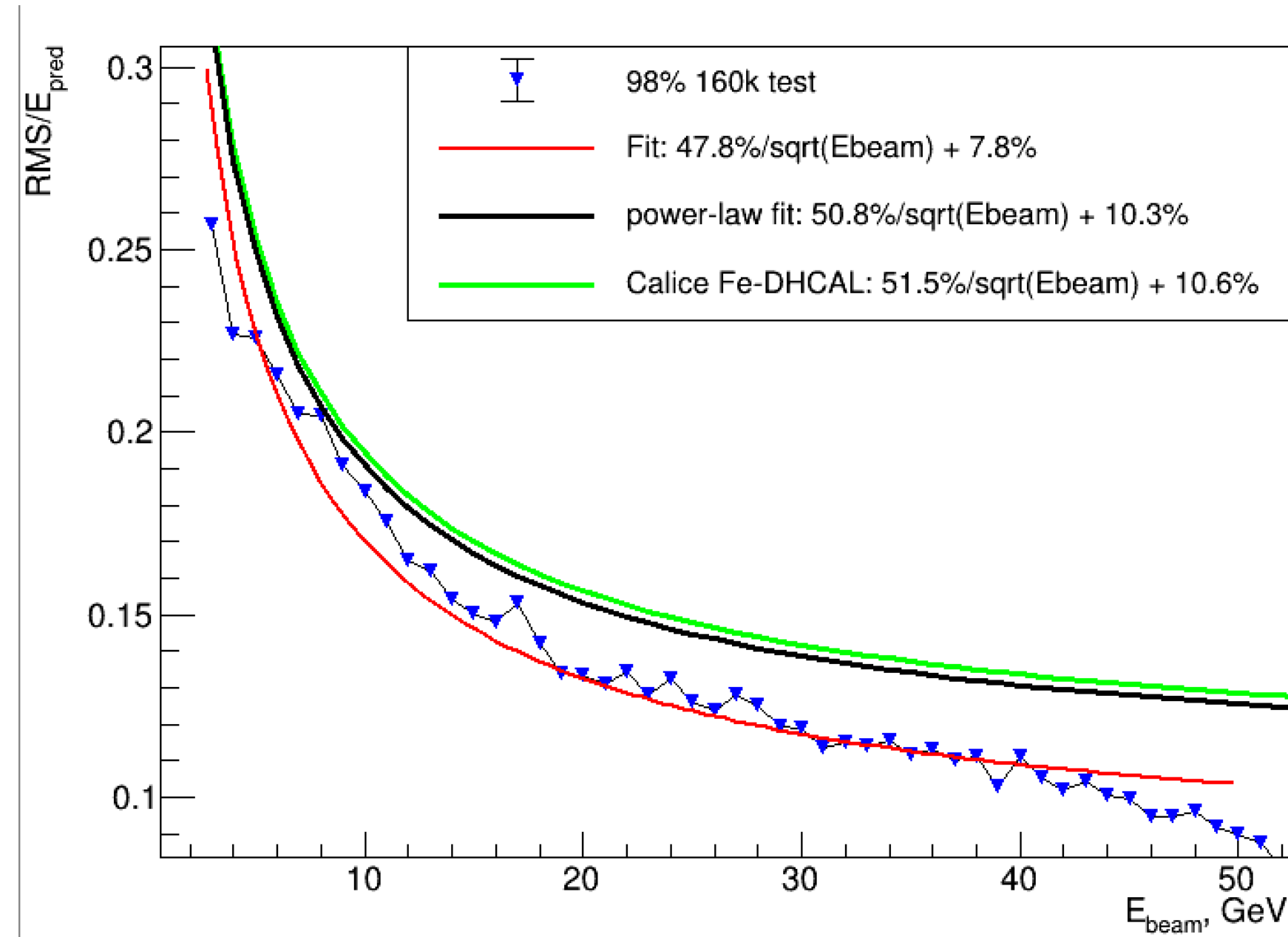


**Table 6:** A summary of the energy resolution of different MIP detection efficiency and average pad-multiplicity values. The energy reconstruction is based on the power-law parametrization. For comparison, the last row includes the results of the CALICE RPC Fe-DHCAL, which includes offline software compensation [20].

Average Pad-Multiplicity	MIP-Detection Efficiency	S [% GeV]	C [%]
1.1	98%*	50.8 + (0.2, -0.3)	10.3 ± 0.06
1.1	95%*	51.1 + (0.3, -0.2)	10.3 ± 0.04
1.1	90%*	50.8 ± 0.2	10.6 ± 0.07
1.1	70%*	51.2 ± 0.2	11.4 ± 0.05
1.6	98%*	48.4 ± 0.3	12.2 ± 0.1
CALICE Fe-DHCAL [20]**	1.69 97%	51.5 ± 1.5	10.6 ± 0.5

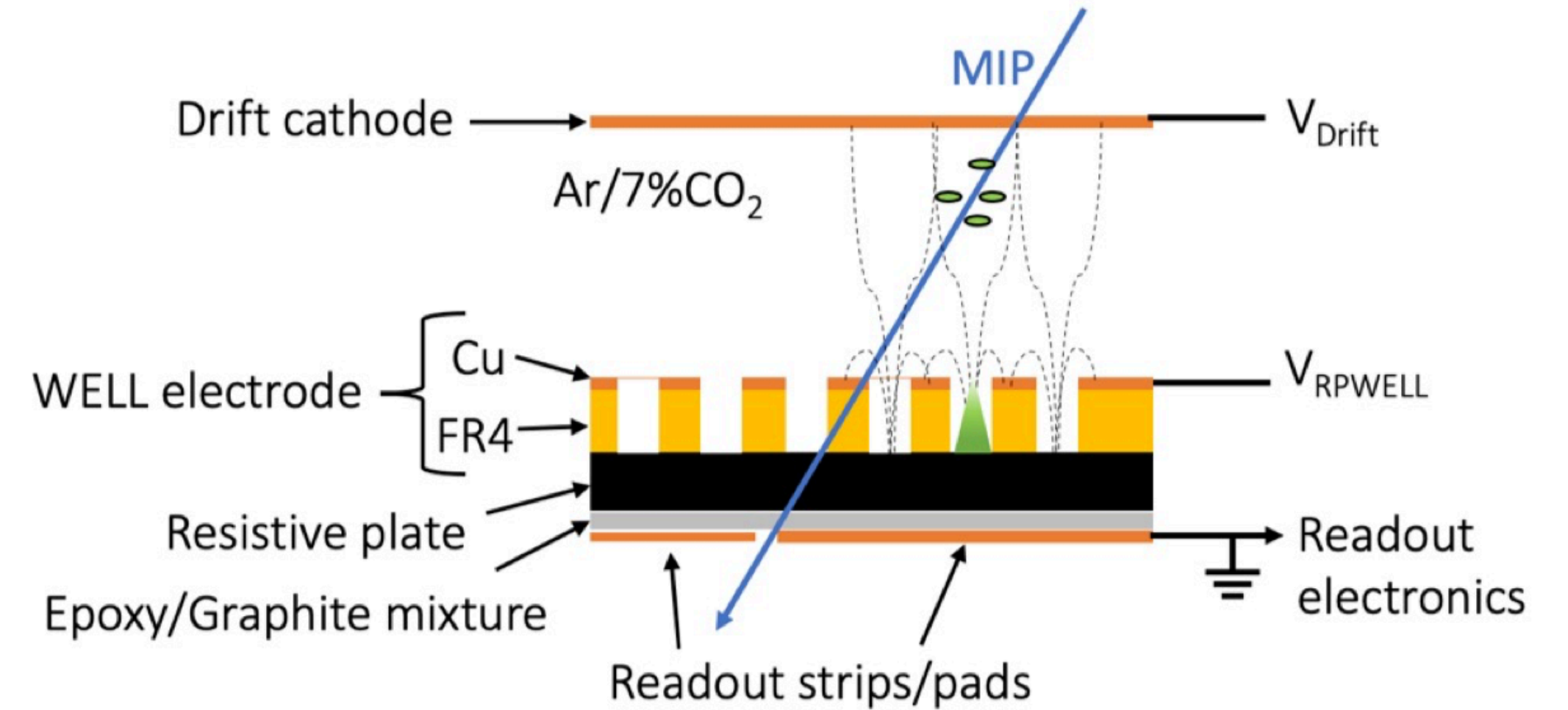
\* Uniform detection efficiency    \*\* Using software compensation

\*\*CALICE collaboration,  
Analysis of Testbeam Data  
of the Highly Granular  
RPC-Steel CALICE Digital  
Hadron Calorimeter and  
Validation of Geant4  
Monte Carlo Models, Nucl.  
Instrum. Meth. A 939  
(2019) 89  
[arXiv:1901.08818].

GNN GAT8:	1.1	98%	50.3+/-1.8	4.0+/-1.6
GNN DS10L:	1.1	98%	47.8+/-0.009	7.8+/-0.003

# Resistive Plate WELL Detector

- Single-sided Thick GEM electrode coupled to the readout anode through high bulk resistivity
  - Combining RPC and MPGD concepts
- Ionization induced primary electrons
  - Drift along the field lines into the THGEM holes
  - Undergo charge avalanche multiplication
- Signals induced on a segmented anode by the movement of charges
- Stable operation at the gain up to a few  $10^3$  and rate up to  $100\text{kHz}/\text{cm}^2$



Potential advantages:

- Operation in environment friendly gases (Ar)
- Industrially produced
- Robustness
- Simple assembly procedure
- Closed geometry

Refs:

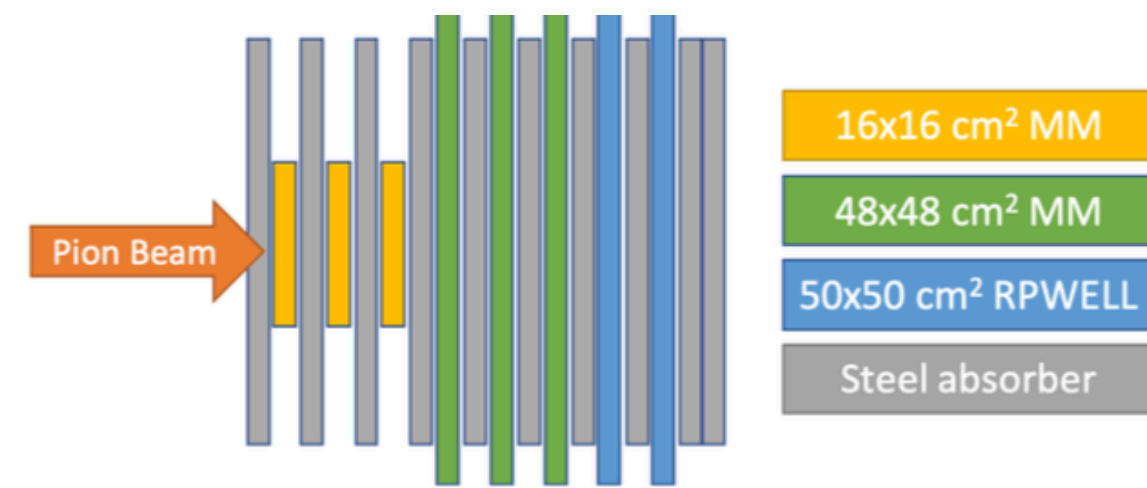
A Rubin et al 2013 JINST 8 P11004

L. Moleri et al 2017 JINST 12 P10017

L. Moleri et al 2016 JINST 11 P09013

<https://doi.org/10.1016/j.nima.2016.06.009>

# Test-beam and simulation studies towards RPWELL-based DHCAL



- Three 16x16 cm<sup>2</sup> resistive Micromegas
- Three 48x48 cm<sup>2</sup> resistive Micromegas
- Two 50x50 cm<sup>2</sup> RPWELLs
- 2 cm thick steel absorbers

